
Summary of Results of NASA F-15 Flight Research Program

**Frank W. Burcham, Jr., Gary A. Trippensee, David F. Fisher,
and Terrill W. Putnam**

April 1986

Summary of Results of NASA F-15 Flight Research Program

Frank W. Burcham, Jr., Gary A. Trippensee, David F. Fisher, and Terrill W. Putnam
Ames Research Center, Dryden Flight Research Facility, Edwards, California

1986



National Aeronautics and
Space Administration

Ames Research Center

Dryden Flight Research Facility
Edwards, California 93523

**SUMMARY OF RESULTS OF NASA F-15
FLIGHT RESEARCH PROGRAM**

Frank W. Burcham, Jr.,* Gary A. Trippensee,**
David F. Fisher,† and Terrill W. Putnam‡
NASA Ames Research Center
Dryden Flight Research Facility
Edwards, California

Abstract

NASA conducted a multidisciplinary flight research program on the F-15 airplane. The program began in 1976 when two preproduction airplanes were obtained from the U.S. Air Force. Major projects involved stability and control, handling qualities, propulsion, aerodynamics, propulsion controls, and integrated propulsion-flight controls. Several government agencies and aerospace contractors were involved. In excess of 330 flights were flown, and over 85 papers and reports were published. This document describes the overall program, the projects, and the key results. The F-15 was demonstrated to be an excellent flight research vehicle, producing high-quality results.

Nomenclature

ADECS	adaptive engine control system	EPR	engine pressure ratio, PT6/PT2
AEDC	Arnold Engineering and Development Center	FDA	fault detection and accommodation
AJ	jet nozzle area	FTIT	fan turbine inlet temperature
BTL	boattail angle	H	altitude
BUC	backup control	HIDEC	highly integrated digital electronic control
CAS	control augmentation system	HiMAT	highly maneuverable aircraft technology
CENC	convergent exhaust nozzle control	L	airplane length
C.I.P.	component improvement program	LOD	light-off detector
CIVV	compressor inlet variable vanes	M	Mach number
Cp	pressure coefficient	N1	fan rotor speed
DEEC	digital electronic engine control	N2	compressor rotor speed
DEFCS	digital electronic flight control system	PB	burner pressure
DTMM	maximum-minimum total pressure distortion factor	PLA	power lever angle
EMD	engine model derivative	PS2	engine-inlet static pressure
<hr/>		PS6	turbine discharge static pressure
<hr/>		PT2	fan inlet total pressure
<hr/>		PT6	mixed turbine discharge total pressure
<hr/>		$\sqrt{\bar{p}_s^2}$	surface pressure root-mean-square pressure fluctuation amplitude
<hr/>		q	dynamic pressure
<hr/>		RCVV	rear compressor variable vanes
<hr/>		Re	Reynolds number
<hr/>		Ret	transition Reynolds number
<hr/>		TT2	engine-inlet total temperature
<hr/>		U	velocity
<hr/>		USAF	U.S. Air Force
<hr/>		WAC	corrected fan airflow
<hr/>		WF	fuel flow
<hr/>		WF GG	gas generator fuel flow

*Assistant Chief, Vehicle Technology Branch,
Member AIAA.

**F-15 Project Manager.

†Aerospace Engineer, Member AIAA.

‡Chief, Vehicle Technology Branch, Member AIAA.

W.T.	wind tunnel
X/L	normalized axial distance
x	axial distance
α	angle of attack
β	angle of sideslip
Δ, δ	change in parameter
ϕ	circumferential angle
ν	kinematic viscosity

Subscripts

e	edge conditions
∞	freestream conditions

Introduction

Flight research is a key tool in validating the methodology of aircraft design and development. Flight data provide the basis for validating analytical design codes, ground test and wind tunnel test techniques, and flight simulation techniques. Flight demonstration is also an important part of the development process in which new concepts must be demonstrated and evaluated before being included in production airplanes.¹

Over the last decades, NASA has maintained a series of programs, in which flight research has been conducted in appropriate areas. In the mid-1970s, the NASA Ames Research Center's Dryden Flight Research Facility (Ames-Dryden), in cooperation with the U.S. Air Force (USAF), acquired two F-15 airplanes and began a multidisciplinary flight research program that continued for almost 10 yr. The F-15 represented a new generation of high-performance airplanes with excellent transonic maneuverability and high thrust-to-weight ratio. Areas of research included basic stability and control, handling qualities, buffet, propulsion system performance, engine-inlet compatibility, inlet-airframe integration, nozzle-afterbody integration, propulsion control, advanced engine development and test, integrated propulsion-flight control, and aerodynamic experiments, including tests of a 10-deg cone and space shuttle tiles. In addition, new cockpit display methods and partial pressure suits were tested, and new measurement systems were tested and evaluated. To provide correlation with the flight data, tests were run on wind tunnel scale models at the NASA Langley Research Center and at the Arnold Engineering and Development Center (AEDC), and the engines were tested at the NASA Lewis Research Center. Other wind tunnel tests were also conducted. In all, about 85 technical reports and papers were published. This document presents a summary of the projects conducted and some of the key results obtained.

Description of the F-15 Airplane

The F-15 (Figs. 1 and 2) is a high-performance air-superiority airplane with a high thrust-to-weight ratio and excellent transonic maneuverability. It is manufactured by McDonnell Aircraft Company and has a maximum Mach number capability of 2.5. The airplane has a low aspect ratio shoulder-mounted wing with 45-deg sweep and twin vertical tails. It is powered by two afterburning turbofan engines, each supplied with air by a variable-geometry inlet. The two airplanes used in the NASA flight research program were the F-15A-2 airplane (serial number 710281), the preproduction propulsion test airplane, and F-15A-8 airplane (serial number 710287), the preproduction high-angle-of-attack and spin test airplane. Both airplanes were single-seat airplanes. The F-15A-2 airplane (Fig. 1) retained the original preproduction wing planform, while the F-15A-8 had raked wingtips (Fig. 2) which is the production configuration.

The F-15 flight control system consists of horizontal tails for pitch control, rolling tails and ailerons for roll, and dual rudders for yaw. A fully mechanical flight control system is augmented by a dual-channel limited-authority analog control augmentation system (CAS) in all axes.

The F-15 inlet (Fig. 3) is a variable-geometry design with external compression. It incorporates variable-capture first ramp, with the cowl hinged at a rotation point as shown in Fig. 3. The second, third, and diffuser ramps are linked together. The bypass door exits air from a throat slot bypass. A digital inlet control system positions the ramps and the bypass as a function of sensed variables.

The F100-PW-100 engine (Fig. 4) powers the F-15 airplane. This engine is a low-bypass afterburning turbofan built by Pratt and Whitney. It features a three-stage fan driven by a two-stage low-pressure turbine and a nine-stage compressor driven by a two-stage high-pressure turbine. The mixed flow augmentor incorporates five segments and a variable-area nozzle. These station designations are also shown in Fig. 4.

Summary of Flight Research Programs

Numerous flight research programs have been conducted using the two F-15 airplanes. The major research programs (Fig. 5) are summarized here and are later discussed in more detail.

F-15A-8 was acquired in 1976 and was used to conduct basic studies of handling qualities, stability and control, aerodynamic buffet, tracking, and overall agility. At the same time, F-15A-2 was flown for an engine-inlet compatibility study. Following completion of this effort, several flights were flown to evaluate changes to the F100 engines in the component improvement program.

F-15A-2 was grounded for an instrumentation phase, and the test engines were taken to NASA Lewis Research Center for calibration tests and evaluation. F-15A-8 was flown during this period by several NASA pilots to evaluate airplane flying qualities characteristics. In mid-1977, F-15A-2 was flown for the evaluation of the inlet-airframe and nozzle-aft-engine interaction characteristics. During this period, the calibrated engines were installed, the in-flight thrust was calculated, and a new thrust calculation algorithm was evaluated. Data were acquired for comparison of wind tunnel and flight measurements, and special flight test techniques were developed to improve the match between wind tunnel and flight test conditions.

In early 1978, the AEDC 10-deg transition cone was mounted on the nose of F-15A-8 and flown at Mach numbers up to 2.0. This cone had been used to calibrate 23 American and European wind tunnels for freestream disturbance levels by measuring the laminar to turbulent transition location. Two years later, a similar cone was flown at a local angle of attack of 11 deg at Mach numbers of 0.6, 1.2, and 1.8. At this angle of attack, symmetric vortices formed on the leeward side of the cone. The pressure distributions and lines of separation were obtained. The data quality was enhanced by the use of special cockpit displays that made it possible to hold very steady flight conditions at high Mach number.

In late 1979, the flight integrity of the space shuttle thermal protection tiles needed to be verified. The F-15A-2 airplane was used, with four different tile samples mounted at various locations on the airplane. As a result of these tests, several changes were made in the tile system. At the same time, an engine-inlet static pressure (PS2) sensor was flown. Following the shuttle tile and PS2 tests, F-15A-2 airplane was retired from service and is now on display at Langley Air Force Base.

In late 1980, on the basis of NASA test experience with the F100 engine, the USAF and Pratt and Whitney expressed interest in a flight evaluation of the newly developed digital electronic engine control (DEEC) system. This engine was installed in the F-15A-8 airplane and flown in a five-phase flight evaluation that continued from 1981 to 1983. During the DEEC testing, an experiment was conducted to evaluate an in-flight structural deflection measuring system. This system was mounted on the right wing of the F-15A-8 airplane and evaluated at a series of flight conditions.

In 1983, the USAF was developing an upgraded model of the F100 engine, the F100 engine model derivative (EMD). Again, the desire for an early flight evaluation led to a joint NASA and USAF program to evaluate the F100 EMD. The tests began in March 1983 and continued into 1986.

In 1985, the Highly Integrated Digital Electronic Control (HIDEC) program was initiated to investigate the benefits of engine-flight control integration. A digital flight control system was developed and tested. The DEEC was modified to accept commands from the HIDEC computer to trade

engine stall margin for increased thrust when the full stall margin was not required. The system was installed in the airplane in early 1986.

Recently, the F-15A-8 airplane was again used in the test-bed role — in this case, to conduct research on supersonic natural laminar flow. A smooth glove was installed on the right wing, and special instrumentation was installed to determine the extent of laminar flow on a swept wing at supersonic speeds. The F-15A-8 airplane was also used to conduct studies on the acoustic characteristics of twin jets.

Flight Test Trajectory Guidance

A capability developed early in the F-15 flight research program has been a key part of the research output of the program. The initial program objectives included several projects in which comparisons of wind tunnel data with flight measurements were required. Previous experience in the YF-12 project pointed out the need for methods to improve the ability to achieve precise flight conditions. Therefore, a technique, called flight test trajectory guidance (Fig. 6), was developed. As shown in Fig. 6(a), telemetry data were received from the airplane, and a series of computations were performed in a ground computer. The appropriate guidance commands were generated and telemetered back to the airplane and displayed in the cockpit. In most cases, the pilot display was a modified course deviation indicator, such as that in Fig. 6(b). This device displayed pitch commands on the horizontal needle, bank angle commands on the vertical needle, and throttle commands on the side indicator. In some cases, additional information was required. For example, Fig. 6(c) shows the cockpit display of true angle of attack, true sideslip angle, true Mach number, engine airflow, and nozzle boattail angle as well. References 2 to 9 describe the flight test trajectory guidance system in more detail and also present the algorithms used to generate the guidance commands.

Stability and Control, Handling Qualities, Buffet, and Tracking

The initial research on F-15A-8 consisted of an evaluation of the stability and control, handling qualities, buffet characteristics, and the overall airplane tracking.^{10,11} Tasks included windup turns, gunsight tracking, and simulated air-to-air combat. Vortex flows that affect the high-angle-of-attack aerodynamics were studied in a water tunnel.¹²

10-Deg Transition Cone Experiment

To evaluate the effects of wind tunnel turbulence on boundary layer transition, the F-15A-8 was used as a test-bed in a unique flight-to-wind-tunnel correlation experiment (Fig. 7). A sharp slender cone with an included angle of 10 deg and a length of approximately 3 ft was mounted on the nose of the F-15A-8 as shown in Figs. 7(a) and 7(b). This cone, known as the AEDC transition cone, was used previously in calibrations of 23 American and European wind tunnels. The same

instrumentation and techniques were used to detect the onset and end of boundary layer transition and to document the pressure fluctuations in the wind tunnel and in flight.

Comparisons of surface pressure fluctuations for flight, lower noise wind tunnels, and higher noise wind tunnels are shown in Fig. 7(c). The pressure fluctuation levels measured in the lower noise wind tunnels are about twice those measured in flight. The higher noise wind tunnel pressure fluctuations are an order of magnitude higher than the in-flight measurements.

Good correlation of the end of transition Reynolds number Re_T was obtained between data from the lower turbulence wind tunnels and flight up to a Mach number of 1.2, as indicated in Fig. 7(d). Above Mach 1.2, however, the correlation deteriorates, with the flight Re_T being 25- to 30-percent higher than the wind tunnel Re_T at Mach 1.6. Additional information on the transition cone tests may be found in Refs. 13 to 18.

10-Deg Cone Separation Experiment

The three-dimensional leeward separation about the 10-deg cone at a local angle of attack of 11 deg was investigated in flight on the F-15A-8; the results are summarized in Fig. 8. A facsimile of the AEDC transition cone was instrumented with static and dynamic pressures, as shown in Fig. 8(a), and the results were compared with wind tunnel data and numerical computations. The test conditions were at Mach 0.6, 1.2, and 1.8 and at Re between 7 and 10×10^6 . Mean and fluctuating surface pressures were measured. By using obstacle blocks, skin friction magnitudes and separation line positions were obtained.

The mean static pressures from flight and wind tunnel were in good agreement. The computed results, as shown in Fig. 8(b), gave similar distributions but were slightly more positive in magnitude. The experimentally determined primary and secondary separation line locations compared closely with wind tunnel and computed results.¹⁹⁻²¹

The use of trajectory guidance was important in maintaining steady test conditions while acquiring data for the slender cone separation experiment. The Mach number, altitude, and angle of attack were maintained within strict limits at supersonic speeds in sustained turns, as indicated in Fig. 8(c).

Engine-Inlet Compatibility Project

There are several key questions in achieving compatibility between engines and inlets. These include the differences between wind tunnel and flight data, the effects of scale, the effects of Reynolds number, and the effects of filter cut-off frequencies used in data analysis. Another unknown is the effect of simulating an actual engine with a "cold pipe" engine simulator. To attempt to answer these questions, a comprehen-

sive joint NASA and USAF project was conducted using the F-15.

Figure 9 outlines the engine-inlet compatibility research project. Data were available for a one-sixth scale model and a full-scale wind tunnel test model. The full-scale wind tunnel test model included a "cold pipe" engine simulator, as well as an actual engine. All three inlets were instrumented with total pressure sensing arrays at the engine face location. Engine face distortion parameters from the wind tunnel tests were computed and compared with flight data. The highest inlet distortion was produced at extreme flight conditions, such as -10-deg angle of attack and 10-deg sideslip. The flight test trajectory guidance technique was used to assist the pilot in attempting to achieve these conditions; an example is shown in Fig. 9(b).

The effects of Reynolds number as a function of model scale size are shown in Fig. 9(c). In general, the effects of increasing scale size and Reynolds number are favorable; pressure recovery increases, and turbulence and distortion decrease. The effects of filter cutoff frequency on the fan distortion and turbulence are shown in Fig. 9(d). The data provide a guide for selecting cutoff frequencies for future designs. Although not shown, the effect of replacing the simulated engine with an actual engine in the full-scale wind tunnel test was to reduce the distortion and improve the engine-inlet compatibility.

Engine fan stability audits were conducted to evaluate the methodology of the engine manufacturers. Fan stalls were encountered at only a few extreme flight conditions. However, at these conditions, the stability audit stall margins were within approximately 5 percent of the measured values. Results are summarized in Refs. 22 and 23.

Engine Calibrations

Two of the F100 engines used in the flight research projects (engines P680059 and P680063) were calibrated at the NASA Lewis Research Center's Propulsion System Laboratory for thrust and airflow.²⁴⁻²⁶ These calibration results were needed for subsequent inlet and nozzle flight research projects. In addition, a simplified gross thrust method and the engine manufacturer's in-flight thrust calculation routine were evaluated in the calibration.²⁷

Inlet-Airframe Integration Research Project

Another objective of the original F-15 program was the flight evaluation of inlet-airframe interactions. Strong and unforeseen inlet-airframe interactions had been observed on the YF-12 program. The F-15 inlet incorporates extensive variable geometry to maximize performance and, hence, provides an excellent research opportunity. Therefore, in a joint project with the USAF, the inlet of the F-15

was instrumented, and extensive evaluation and comparison with the analytical and wind tunnel data were conducted (Fig. 10).²⁸⁻³⁰

The wind tunnel model used in the project is shown in Fig. 10(a). It featured a complete airplane model with flowing inlets. The left inlet was mounted on a force balance, the right inlet was pressure instrumented, and the entire model was mounted on a force balance. The airplane was instrumented with pressure ports located at the same position as on the one-sixth scale model. The pressure integration routines were carefully coordinated between the wind tunnel and flight data analyses.

Typical results are shown in Fig. 10(b) in which the inlet lift and drag for the wind tunnel pressure integrated and force balance data are compared with the flight data for a range of Mach numbers. The inlet drag measured in flight was lower than the wind tunnel data, while the inlet lift was in good agreement. The flight-determined total inlet drag is shown in Fig. 10(c) and indicates the relative values of drag from the various sources. These results provided one of the first flight determinations of inlet drag.

Nozzle and Aft Engine Integration

The nozzle and aft engine integration results are summarized in Fig. 11. The left engine nozzle and afterbody were extensively instrumented with over 90 orifices, as indicated in Fig. 11(a). These orifice locations matched those of the 1/12th scale wind tunnel model tested at NASA Langley Research Center. Results are presented in Refs. 31 to 36. A typical comparison of flight to wind tunnel data at one orifice row, illustrated in Fig. 11(b), shows good agreement at Mach 0.6, and poorer agreement at Mach 0.9 and 1.2.

The overall nozzle drag, or axial force, plotted in Fig. 11(c), shows the strong effect of Mach and boattail angle. The variation of nozzle drag with Re in Fig. 11(d) shows the drag coefficient decreasing as Re increases. It was found that the effect of the faired-over inlets on the wind tunnel model was affecting the vortex flow over the upper part of the airplane and affecting the flow quality at the nozzle.

In-Flight Thrust

The two F100 engines that had been calibrated at the NASA Lewis Research Center were flown in the F-15. These engines (P680059 and P680063) were instrumented to provide input data for the simplified gross thrust method and the in-flight thrust calculation method. Results³⁷ showed that the simplified gross thrust method was a suitable alternative to more complex methods for determining in-flight gross thrust.

Shuttle Thermal Protection System Evaluation

During the first ferry flight of the space shuttle orbiter, Columbia, on the top of the Boeing 747 carrier aircraft, some of the thermal

protection system tiles and gap fillers loosened or migrated. This unanticipated occurrence at modest flight conditions initiated a reassessment of the effects of airloads on the thermal protection system during launch and reentry.

F-15A-2 aircraft was used to assist in certification of the tiles prior to the first shuttle launch (Fig. 12). In-flight aerodynamic loads tests of four shuttle tile areas, shown in Fig. 12(a), were conducted. The objective of the tests was to demonstrate the performance of the tiles and gap fillers at dynamic pressures up to 1.4 times the predicted launch loads. The four articles tested on the F-15A-2 aircraft were mounted in two separate locations, as indicated in Fig. 12(b). Three test articles were mounted on the right wing, and the other was mounted on the left wing glove. The wing leading edge, window post, and vertical stabilizer tile articles were mounted on the wing; Fig. 12(c) shows the vertical stabilizer article. The shuttle wing glove test article was mounted on the F-15A-2 wing glove, as shown in Fig. 12(d).

Flight test trajectory guidance was used to assist the pilot in flying flight profiles that would provide the proper simulated airloads to the test articles. The test results provided a data base for the verification of wind tunnel data and analytical predictions. In general, the F-15A-2 simulations of the predicted maximum airloads expected on the shuttle were good. The testing did reveal two deficiencies that required redesign. The gap filler assembly and the tile carrier plate assembly were redesigned. Also, a modification of the window post closeout tile was made because the pressure under the window post was higher than predicted. Both modifications were tested on the F-15A-2, and modifications were accomplished on the shuttle prior to its first flight.³⁸

Engine-Inlet Static Pressure

Engine-inlet pressure is a key parameter needed for control of advanced engines. This parameter may be measured directly by total pressure probes; however, total pressure distortion introduces wide variations in the readings or requires a large number of measurements to be made. An alternative is to measure static pressure. Wall static pressures also are sensitive to distortion; however, a stream static pressure at the engine hub has shown promise of providing a useful engine control signal. Therefore, NASA, in conjunction with Pratt and Whitney, has conducted studies³⁹⁻⁴¹ of an engine inlet static pressure (PS2) probe (Fig. 13).

Figure 13(a) shows the hemispherical head PS2 probe on the F100 engine. A 35-probe total pressure array was installed in the engine-inlet guide vanes to provide a correlation with the PS2 probe, as indicated in Fig. 13(b). The ratio of the average fan inlet total pressure (PT2) to PS2 was determined in a number of flights. A manual inlet control system was used to move the inlet ramps to off-schedule positions to increase distortion up to the point of engine stall. Typical

results are shown in Fig. 13(c). The effects of distortion produce a repeatable change in the ratio of the average PT2 to PS2, thus providing a very useful control system signal that is used in the DEEC.

DEEC Evaluation

The DEEC is a full-authority digital system developed to replace the hydromechanical unified fuel control and the supervisory engine electronic control on the F100 engine. The DEEC (Fig. 14) was installed on an F100 engine and flown in the F-15A-8 in a five-phase joint NASA, USAF, and Pratt and Whitney evaluation.⁴²⁻⁶⁷ The DEEC provides control of the compressor inlet variable vanes (CIVV), the rear compressor variable vanes (RCVV), the start bleeds, the main combustor fuel flow, the augmentor fuel flow, and the variable area nozzle, as indicated in Fig. 14(a). The DEEC is a single-channel system with selected input-output redundancy and a simple independent hydromechanical backup control, as shown in Fig. 14(b).

The DEEC incorporates closed-loop control of engine pressure ratio (EPR) and airflow. This eliminates the need for periodic ground trim runs to keep the engine operating within desired limits. It also provides closed-loop starting capability. This capability allowed the F100 astart envelope to be improved as shown in Fig. 14(c), with airspeed reductions of 75 knots.

The DEEC also incorporates improved augmentor control that results in significant improvements in augmentor lighting capability. Figure 14(d) shows the high-altitude low-airspeed idle-to-maximum power throttle transient success at the end of the fourth phase of testing, and also shows the lines of success from previous tests. The overall improvement is in excess of 10,000 ft. The occurrence of augmentor associated stalls was greatly reduced.

In addition, the DEEC has extensive fault detection and accommodation (FDA) capability. In excess of 160 faults can be detected, and many of these can be accommodated by an alternate logic path or reduced capability operation. To evaluate the FDA capability in flight, a series of valves and switches were installed on the engine to introduce simulated failures to the DEEC in flight, as indicated in Fig. 14(e). The FDA logic was evaluated over the test conditions shown in Fig. 14(f) in the fifth phase of DEEC testing. Several problems were identified in detecting failures but, once detected, operation with failed sensors was very successful.

The DEEC evaluation was highly successful, leading to full-scale development and production of an improved version of the F100, the F100-PW-220 engine.

Deflection Measuring System

During the DEEC evaluation, a brief flight evaluation of a deflection measuring system was conducted. This system, designed to provide direct readout of structural deflections, was needed for

the highly maneuverable aircraft technology (HiMAT) and X-29 programs, in which composite structural materials and aeroelastic tailoring were employed. The F-15A-8 was used to develop, check out, and evaluate the operation of the deflection measurement system. The system flown on the F-15A-8 (Fig. 15), consisted of light-emitting diode targets and diode receiver array mounted on the F-15 wing upper surface, as indicated in Fig. 15(a). The upper wing was painted black to minimize the effects of sunlight on the system. The schematic view of the system in Fig. 15(b) shows the light-emitting diode targets that are sequentially illuminated and the diode receiver that senses the deflection. The system was checked out at various levels of normal acceleration and was validated for the HiMAT and X-29 programs.

F100 EMD Flight Evaluation

An advanced version of the F100 engine, the F100 EMD was evaluated in the F-15A-8. The EMD program is a USAF program to provide significant improvements to existing engines. The USAF developed the F100 EMD, in conjunction with Pratt and Whitney (company designation PW1128), and formulated a joint program with NASA to conduct a flight evaluation (Fig. 16). The advanced features of the F100 EMD, shown in Fig. 16(a), include a redesigned fan with higher airflow and pressure ratio, a revised combustor, single crystal turbine blades and vanes, a DEEC, and a redesigned 16-segment augmentor.

The F100 EMD engine has about 15 percent more thrust than the standard F100. This improves the performance of the F-15 significantly. Figure 16(b) shows that the time to accelerate from Mach 0.8 to 2.0 is reduced by 25 percent. The airplane also has supersonic cruise capability (Mach 1.15) at intermediate power with the F100 EMD engines. The 16-segment augmentor, which replaced the 5-segment augmentor of the F100, exhibited improved operation. The smaller pressure pulses associated with the more numerous segments completely eliminated augmentor induced stalls in the flight evaluation, as indicated in Fig. 16(c).

During the flight evaluation, compressor stalls were encountered during intermediate-to-idle power throttle transients at extremely high-altitude and low-airspeed conditions. These stalls were not predicted by analytical or altitude facility test results. Special high-response pressure probes were installed at the fan discharge; they demonstrated that, under certain conditions, flow separation occurred and resulted in increased distortion to the compressor. The reason that the altitude facility results could not duplicate the flight results is not clear. More information on the F100 EMD evaluation is presented in Refs. 68 to 71.

HIDEC Project

The objective of the HIDEC project is to evaluate the performance improvements and mission effectiveness increases that result from propulsion and flight control integration.⁷²⁻⁸⁶ This will be accomplished on the F-15A-8 by integra-

ting the flight control and engine control systems (Fig. 17). As shown in Fig. 17(a), the F-15A-8 has been equipped with a digital electronic flight control system (DEFCS), the F100 EMD engines with DEECs, and digital interface and bus control equipment to permit the flight controls and engine controls to communicate. An uplink from ground-based computers permits control computations to be made in general-purpose computers in higher order languages and then uplinked to the airplane.

One of the HIDECS modes is an adaptive engine control system (ADECS) mode in which engine stall margin is traded for increased performance as a function of flight conditions. Typically, engine stall margin is set to accommodate the worst case combination of engine and inlet generated disturbances. When either the engine or inlet disturbances are less severe, additional performance may be obtained in the form of increased thrust, decreased fuel consumption, or increased engine life. Figure 17(b) shows a block diagram of the ADECS mode. Inputs from the DEFCS representing airplane attitudes, rates, and pilot inputs are used to compute the current and predicted inlet distortion and, hence, the fan stall margin requirements. The DEEC provides information on the engine status from which the required stall margin is computed. The allowable EPR is calculated, and the difference between the current and the allowable EPR is then transmitted to the DEEC. Thrust increases are predicted to be in the 5- to 10-percent range, with fuel flow reductions in the 5- to 15-percent range, as shown in Figs. 17(c) and 17(d).

Supersonic Laminar Flow

The occurrence of natural laminar flow on airfoils is of interest in drag reduction efforts. In particular, there is little or no information on the extent of natural laminar flow on swept wings at supersonic speeds. The F-15A-8 was used as a test-bed airplane to investigate supersonic laminar flow (Fig. 18). A very smooth fiberglass glove was installed on the leading edge of the right wing, as shown in Fig. 18(a). Pressure instrumentation installed in the glove measures the pressure gradient, and hot film anemometers were used to determine the extent of laminar flow, as indicated in Fig. 18(b). Flight results confirmed that small amounts of natural laminar flow exist at supersonic speeds at certain conditions.

High-Altitude Partial Pressure Protective System

As an alternative to cumbersome pressure suits, the Royal Air Force high-altitude partial pressure protective system (jerkin) was evaluated in the F-15A-8 (Fig. 19). The jerkin system, shown in Fig. 19(a), consists of a pressure jerkin torso garment, anti-gravity trousers, a pressure demand mask, and a pressure regulator. The system⁸⁷ provides the pilot with safe get-down capability in case of cockpit depressurization at altitudes up to 60,000 ft, as indicated in Fig. 19(b). The jerkin has been used for flights at high altitudes in the supersonic laminar flow project and in high-altitude engine and augmentor evaluations.

Flight and Publication Rates

The flight rates of F-15A-2 and F-15A-8 are shown in Fig. 20. Prior to its retirement, F-15A-2 flew 140 research flights with an average of 28 flights/yr. F-15A-8 has flown 193 flights for an average of 19 research flights/yr. There has been increasing use of aerial refueling to extend flight times in the latter years.

The publication rate (reference reports and papers) was approximately 6/yr for the first 6 yr and has increased to approximately 19/yr for the last 3 yr.

Summary

A 10-yr flight research program has been conducted at NASA Ames-Dryden with the F-15 airplane. More than 330 flights have been flown, and over 85 reports and papers have been published. The F-15 has been demonstrated to be a versatile and effective airplane for a wide variety of flight experiments. The results have been used to provide early insight into problems before new systems are committed to production. It has served as an effective way to transition technology into operational use. Results have been used to verify and validate some currently used test techniques, as well as to point out limitations and weaknesses in some areas. Flight test trajectory guidance techniques that have been developed have increased the quality of data for this and other flight research programs. The F-15 has served as a test-bed for proving advanced equipment for other flight vehicles and for carrying basic aerodynamic experiments into the true flight environment.

Acknowledgment

The F-15 research program was sponsored by the NASA Office of Aeronautics and Space Technology, High-Speed Aircraft Division, Jack Levine, Manager.

References

¹Szalai, K.J., "Role of Research Aircraft in Technology Development," AIAA Paper 84-2473, Nov. 1984.

Trajectory Guidance

²Swann, M.R., Duke, E.L., Enevoldson, E.K., and Wolf, T.D., "Experience With Flight Test Trajectory Guidance," AIAA Paper 81-2504, Nov. 1981.

³Walker, R.A. and Gupta, N.K., "Flight Test Trajectory Control Analysis," NASA CR-170395, 1983.

⁴Duke, E.L., Swann, M.R., Enevoldson, E.K., and Wolf, T.D., "Experience With Flight Test Trajectory Guidance," J. Guidance, Control, and Dynamics, vol. 6, no. 5, Sept.-Oct. 1983, pp. 393-398.

⁵Walker, R.A., Gupta, N.K., Duke, E.L., and Patterson, B., "Developments in Flight Test Trajectory Control," AIAA Paper 84-0240, Jan. 1984.

⁶Menon, P.K.A., Saberi, H.A., Walker, R.A., and Duke, E.L., "Flight Test Trajectory Controller Synthesis With Constrained Eigenstructure Assignment," American Control Conference Proc., vol. 3, June 1985, pp. 1181-1186.

⁷Alag, G.S. and Duke, E.L., "Development of Control Laws for a Flight Test Maneuver Autopilot for an F-15 Aircraft," NASA TM-86736, 1985.

⁸Duke, E.L. and Antoniewicz, R.F., "Development and Validation of a General Purpose Linearization Program for Rigid Aircraft Models," NASA TM-86737, 1985.

⁹Alag, G.S. and Duke, E.L., "Development of a Flight Test Maneuver Autopilot for an F-15 Aircraft," NASA TM-86799, 1985.

Stability and Control, Handling Qualities, Buffet, and Tracking

¹⁰Sisk, T.R., "A Technique for the Assessment of Fighter Aircraft Precision Controllability," AIAA Paper 78-1364, Aug. 1978.

¹¹Sisk, T.R. and Matheny, N.W., "Precision Controllability of the F-15 Airplane," NASA TM-72861, 1979.

¹²Lorincz, D.J. and Friend, E.L., "Water Tunnel Visualization of the Vortex Flows of the F-15," AIAA Paper 79-1649, Aug. 1979.

10-Deg Transition Cone

¹³Dougherty, N.S., Jr. and Fisher, D.F., "Boundary Layer Transition on a 10-Degree Cone: Wind Tunnel/Flight Data Correlation," AIAA Paper 80-0154, Jan. 1980.

¹⁴Saltzman, E.J. and Ayers, T.G., "A Review of Flight-to-Wind Tunnel Drag Correlation," AIAA Paper 81-2475, Nov. 1981.

¹⁵Dougherty, N.S., Jr. and Fisher, D.F., "Boundary-Layer Transition Correlation on a Slender Cone in Wind Tunnels and Flight for Indications of Flow Quality," NASA TM-84732, 1982.

¹⁶Fisher, D.F. and Dougherty, N.S., Jr., "In-Flight Transition Measurement on a 10° Cone at Mach Numbers From 0.5 to 2.0," NASA TP-1971, 1982.

¹⁷Fisher, D.F. and Dougherty, N.S., Jr., "Flight and Wind-Tunnel Correlation of Boundary-Layer Transition on the AEDC Transition Cone," Ground/Flight Test Techniques and Correlations, AGARD CP-339, Oct. 1982, pp. 5-1 to 5-25.

¹⁸Fisher, D.F. and Dougherty, N.S., Jr., "Flight and Wind-Tunnel Correlation of Boundary-Layer Transition on the AEDC Transition Cone," NASA TM-84902, 1982.

10-Deg Cone Separation

¹⁹McRae, D.S., Peake, D.J., and Fisher, D.F., "A Computational and Experimental Study of High Reynolds Number Viscous/Inviscid Interaction About a Cone at High Angle of Attack," AIAA Paper 80-1422, July 1980.

²⁰Peake, D.J., Fisher, D.F., and McRae, D.S., "Flight Experiments With a Slender Cone at Angle of Attack," AIAA Paper 81-0337, Jan. 1981.

²¹Peake, D.J., Fisher, D.F., and McRae, D.S., "Flight, Wind Tunnel, and Numerical Experiments With a Slender Cone at Incidence," AIAA J., vol. 20, no. 10, Oct. 1982, pp. 1338-1345.

Engine-Inlet Compatibility

²²Stevens, C.H., Spong, E.D., and Hammock, M.S., "F-15 Inlet/Engine Test Techniques and Distortion Methodologies Studies," NASA CR-144866, 1978.

²³Stevens, C.H., Spong, E.D., Nugent, J., and Neumann, H.E., "Reynolds Number, Scale, and Frequency Content Effects on F-15 Instantaneous Distortion," AIAA Paper 79-0104, Jan. 1979.

Engine Calibrations

²⁴Kurtenbach, F.J., "Comparison of Calculated and Altitude-Facility-Measured Thrust and Airflow of Two Prototype F100 Turbofan Engines," NASA TP-1373, 1978.

²⁵Biesiadny, T.J., Lee, D., and Rodriguez, J.R., "Airflow and Thrust Calibration of an F100 Engine, S/N P680059, at Selected Flight Conditions," NASA TP-1069, 1978.

²⁶Biesiadny, T.J., Lee, D., and Rodriguez, J.R., "Altitude Calibration of an F100, S/N P680063, Turbofan Engine," NASA TP-1228, 1978.

²⁷Kurtenbach, F.J., "Evaluation of a Simplified Gross Thrust Calculation Technique Using Two Prototype F100 Turbofan Engines in an Altitude Facility," NASA TP-1482, 1979.

Inlet-Airframe Integration

²⁸Webb, L.D., Whitmore, S.A., and Janssen, R.L., "Preliminary Flight and Wind Tunnel Comparisons of the Inlet/Airframe Interaction of the F-15 Airplane," AIAA Paper 79-0102, Jan. 1979.

²⁹Webb, L.D. and Nugent, J., "Results of the F-15 Propulsion Interactions Program," AIAA Paper 82-1041, June 1982.

³⁰Webb, L.D., Andriyich-Varda, D., and Whitmore, S.A., "Flight and Wind-Tunnel Comparisons of the Inlet/Airframe Interaction of the F-15 Airplane," NASA TP-2374, 1984.

Nozzle and Aft Engine Integration

- 31Nugent, J., Taillon, N.V., and Pendergraft, O.C., Jr., "Status of a Nozzle-Airframe Study of a Highly Maneuverable Fighter," AIAA Paper 78-990, July 1978.
- 32Plant, T.J., Nugent, J., and Davis, R.A., "Flight-Measured Effects of Boattail Angle and Mach Number on the Nozzle Afterbody Flow of a Twin-Jet Fighter," AIAA Paper 80-0110, Jan. 1980.
- 33Nugent, J., Plant, T.J., Davis, R.A., and Taillon, N.V., "Pressures Measured in Flight on the Aft Fuselage and External Nozzle of a Twin-Jet Fighter," NASA TP-2017, 1983.
- 34Pendergraft, O.C., Jr. and Carson, G.T., Jr., "Fuselage and Nozzle Pressure Distributions of a 1/12-Scale F-15 Propulsion Model at Transonic Speeds," NASA TP-2333, 1984.
- 35Pendergraft, O.C., Jr. and Nugent, J., "Results of a Wind Tunnel/Flight Test Program To Compare Afterbody/Nozzle Pressures on a 1/12 Scale Model and an F-15 Aircraft," SAE Paper 84-1543, Oct. 1984.
- 36Nugent, J. and Pendergraft, O.C., Jr., "Comparison of Wind Tunnel and Flight Test Afterbody and Nozzle Pressures for a Twin-Jet Fighter Aircraft at Transonic Speeds," NASA TP-2588, 1986.

In-Flight Thrust

- 37Kurtenbach, F.J. and Burcham, F.W., Jr., "Flight Evaluation of a Simplified Gross Thrust Calculation Technique Using an F100 Turbofan Engine in an F-15 Airplane," NASA TP-1782, 1981.

Shuttle Tiles

- 38Meyer, R.R., Jr., Jarvis, C.R., and Barneburg, Jack, "In-Flight Aerodynamic Load Testing of the Shuttle Thermal Protection System," AIAA Paper 81-2468, Nov. 1981.

Engine-Inlet Static Pressure

- 39Foote, C.H. and Jaekel, R.J., "Flight Evaluation of an Engine Static Pressure Noseprobe in an F-15 Airplane," NASA CR-163109, 1981.

- 40Hughes, D.L., Myers, L.P., and Mackall, K.G., "Effects of Inlet Distortion on a Static Pressure Probe Mounted on the Engine Hub in an F-15 Airplane," Digital Electronic Engine Control (DEEC) Flight Evaluation in an F-15 Airplane, NASA CP-2298, 1984, pp. 73-89.

- 41Hughes, D.L., Myers, L.P., and Mackall, K.G., "Effects of Inlet Distortion on a Static Pressure Probe Mounted on the Engine Hub in an F-15 Airplane," NASA TP-2411, 1985.

DEEC

- 42Barrett, W.J., Rembold, J.P., Burcham, F.W., Jr., and Myers, L.P., "Flight Test of a Full

Authority Digital Electronic Engine Control System in an F-15 Aircraft," AIAA Paper 81-1501, July 1981.

43Burcham, F.W., Jr., Myers, L.P., Nugent, J., Lasagna, P., and Webb, L.D., "Recent Propulsion System Flight Tests at NASA Dryden Flight Research Center," AIAA Paper 81-2438, Nov. 1981.

44Myers, L., Mackall, K., Burcham, F.W., Jr., and Walter, W., "Flight Test Results of a Digital Electronic Engine Control System in an F-15 Airplane," AIAA Paper 82-1080, June 1982.

45Barrett, W.J., Rembold, J.P., Burcham, F.W., Jr., and Myers, L.P., "Digital Electronic Engine Control System - F-15 Flight Test," J. Aircraft, vol. 20, no. 2, Feb. 1983, pp. 134-141.

46Licata, S.J. and Burcham, F.W., Jr., "Airstart Performance of a Digital Electronic Engine Control System in an F-15 Airplane," NASA TM-84908, 1983.

47Kock, B.M., "Digital Electronic Engine Control F-15 Overview," Digital Electronic Engine Control (DEEC) Flight Evaluation in an F-15 Airplane, NASA CP-2298, 1984, pp. 1-14.

48Putnam, T.W., "Digital Electronic Engine Control History," Digital Electronic Engine Control (DEEC) Flight Evaluation in an F-15 Airplane, NASA CP-2298, 1984, pp. 15-31.

49Myers, L.P., "F-15 Digital Electronic Engine Control System Description," Digital Electronic Engine Control (DEEC) Flight Evaluation in an F-15 Airplane, NASA CP-2298, 1984, pp. 33-53.

50Werner, R.A., Willoch, R.G., Jr., and Abdelwahab, M., "NASA Lewis F100 Engine Testing," Digital Electronic Engine Control (DEEC) Flight Evaluation in an F-15 Airplane, NASA CP-2298, 1984, pp. 55-71.

51Myers, L.P., "Flight Testing the Digital Electronic Engine Control in the F-15 Airplane," Digital Electronic Engine Control (DEEC) Flight Evaluation in an F-15 Airplane, NASA CP-2298, 1984, pp. 91-105.

52Baer-Riedhart, J.L., "Digital Electronic Engine Control Fault Detection and Accommodation Flight Evaluation," Digital Electronic Engine Control (DEEC) Flight Evaluation in an F-15 Airplane, NASA CP-2298, 1984, pp. 107-126.

53Walsh, K.R. and Burcham, F.W., Jr., "Flight Evaluation of a Hydromechanical Backup Control for the Digital Electronic Engine Control System in an F100 Engine," Digital Electronic Engine Control (DEEC) Flight Evaluation in an F-15 Airplane, NASA CP-2298, 1984, pp. 141-155.

54Johnson, J.B., "Backup Control Airstart Performance on a Digital Electronic Engine Control-Equipped F100 Engine," Digital Electronic Engine Control (DEEC) Flight Evaluation in an F-15 Airplane, NASA CP-2298, 1984, pp. 157-170.

- 55**Ray, R.J. and Myers, L.P., "Real-Time In-Flight Thrust Calculation on a Digital Electronic Engine Control-Equipped F100 Engine in an F-15 Airplane," Digital Electronic Engine Control (DEEC) Flight Evaluation in an F-15 Airplane, NASA CP-2298, 1984, pp. 215-230.
- 56**Putnam, T.W., Burcham, F.W., Jr., and Kock, B.M., "Flight Testing the Digital Electronic Engine Control (DEEC) - A Unique Management Experience," 14th Annual SFTE Symposium Proc., 1983, pp. 2.2-1 to 2.2-6.
- 57**Myers, L.P. and Burcham, F.W., Jr., "Comparison of Results Obtained From Flight Tests and Simulated Tests of a Digital Electronic Engine Control System in an F-15 Airplane," NASA TM-84903, 1983.
- 58**Burcham, F.W., Jr., Myers, L.P., and Walsh, K.R., "Flight Evaluation Results for a Digital Electronic Engine Control in an F-15 Airplane," AIAA Paper 83-2703, Nov. 1983.
- 59**Johnson, J.B. and Nelson, J., "Flight Evaluation of the DEEC Secondary Engine Control Air-Start Capability," NASA TM-84910, 1983.
- 60**Burcham, F.W., Jr., Myers, L.P., and Zeller, J.R., "Flight Evaluation of Modifications to a Digital Electronic Engine Control System in an F-15 Airplane," NASA TM-83088, 1983.
- 61**Burcham, F.W., Jr., "Airstart Performance of a Digital Electronic Engine Control System on an F100 Engine," Digital Electronic Engine Control (DEEC) Flight Evaluation in an F-15 Airplane, NASA CP-2298, 1984, pp. 127-139.
- 62**Burcham, F.W., Jr., and Pai, G.D., "Augmentor Transient Capability of an F100 Engine Equipped With a Digital Electronic Engine Control," Digital Electronic Engine Control (DEEC) Flight Evaluation in an F-15 Airplane, NASA CP-2298, 1984, pp. 171-199.
- 63**Burcham, F.W., Jr. and Zeller, J.R., "Investigation of a Nozzle Instability on an F100 Engine Equipped With a Digital Electronic Engine Control," Digital Electronic Engine Control (DEEC) Flight Evaluation in an F-15 Airplane, NASA CP-2298, 1984, pp. 201-214.
- 64**Ray, R.J., "In-Flight Thrust Determination on a Real-Time Basis," M.S. Thesis, California Polytechnic Univ., San Luis Obispo, Apr. 1984.
- 65**Digital Electronic Engine Control (DEEC) Flight Evaluation in an F-15 Airplane, NASA CP-2298, 1984.
- 66**Myers, L.P., Baer-Riedhart, J.L., and Maxwell, M.D., "Fault Detection and Accommodation Testing on an F100 Engine in an F-15 Airplane," NASA TM-86735, 1985.
- 67**Burcham, F.W., Myers, L.P., and Walsh, K.R., "Flight Evaluation of a Digital Electronic Engine Control in an F-15 Airplane," J. Aircraft, vol. 22, no. 12, Dec. 1985, pp. 1072-1078.
- F100 EMD**
- 68**Myers, L.P., and Burcham, F.W., Jr., "Preliminary Flight Test Results of the F100 EMD Engine in an F-15 Airplane," NASA TM-85902, 1984.
- 69**Cho, T.K. and Burcham, F.W., Jr., "Preliminary Flight Evaluation of F100 Engine Model Derivative Airstart Capability in an F-15 Airplane," NASA TM-86031, 1984.
- 70**Crawford, D.B. and Burcham, F.W., Jr., "Effect of Control Logic Modifications on Airstart Performance of F100 Engine Model Derivative Engines in an F-15 Airplane," NASA TM-85900, 1984.
- 71**Walton, J.T. and Burcham, F.W., Jr., "Augmentor Performance of an F100 Engine Model Derivative Engine in an F-15 Airplane," NASA TM-86745, 1986.
- HIDEC**
- 72**Burcham, F.W., Jr., "Propulsion-Flight Control Integration Technology," Active Controls in Aircraft Design, AGARD AG-234, Nov. 1978, pp. 7-1 to 7-9.
- 73**Carlin, C.M. and Hastings, W.J., "Propulsion/Flight Control Integration Technology (PROFIT) Design Analysis Status," NASA CR-144875, 1978.
- 74**Carlin, C.M. and Hastings, W.J., "Propulsion/Flight Control Integration Technology (PROFIT) Software System Definition," NASA CR-144876, 1979.
- 75**Burcham, F.W., Jr. and Stewart, J.F., "The Development Process for Integrated Propulsion-Flight Controls," Tactical Aircraft Research and Technology, NASA CP-2162, Part 1, 1980.
- 76**Yonke, W.A., "Integrated Flight/Propulsion Control: HIDEC Modes," MCAIR 84-011, McDonnell Douglas Corp., 1984.
- 77**Burcham, F.W., Jr. and Haering, E.A., Jr., "Highly Integrated Digital Engine Control System on an F-15 Airplane," NASA TM-86040, 1984.
- 78**Myers, L.P. and Burcham, F.W., Jr., "Propulsion Control Experience Used in the Highly Integrated Digital Electronic Control (HIDEC) Program," NASA TM-85914, 1984.
- 79**Baer-Riedhart, J.L. and Landy, R.J., "Highly Integrated Digital Electronic Control - Digital Flight Control, Aircraft Model Identification and Adaptive Engine Control," AIAA Paper 85-1877, Aug. 1985.
- 80**Haering, E.A., Jr. and Burcham, F.W., Jr., "Minimum Time and Fuel Flight Profiles for an F-15 Airplane With a Highly Integrated Digital Electronic Control System," NASA TM-86042, 1984.
- 81**Burcham, F.W., Jr., Myers, L.P., and Ray, R.J., "Predicted Performance Benefits of an Adaptive Digital Engine Control System on an F-15 Airplane," NASA TM-85916, 1985.

82 "Digital Electronic Engine Controls Examined," *Aerosp. Eng.*, vol. 5, no. 2, Feb. 1985, pp. 34-38.

83 Ogborn, S., "State Variable Dynamic Model of a PW1128 Engine With a DEEC Control," P&W FR-18761A, Pratt and Whitney, 1985.

84 Yonke, W.A., Terrell, L.A., and Myers, L.P., "Integrated Flight/Propulsion Control: Adaptive Engine Control System Mode," AIAA Paper 85-1425, July 1985.

85 Putnam, T.W., Burcham, F.W., Jr., Andries, M.G., and Kelly, J.B., "Performance Improvements of a

Highly Integrated Digital Electronic Control System for an F-15 Airplane," NASA TM-86748, 1985.

86 Andries, M.G. and Terrell, L.A., "Highly Integrated Digital Electronic Control HIDECA Sea Level Test Report for Engine P085-11," P&W FR-19248, Pratt and Whitney, 1986.

High-Altitude Partial Pressure Protective System

87 Ashworth, G.R., Putnam, T.W., Dana, W.J., Enevoldson, E.K., and Winter, W.R., "Flight Test Evaluation of an RAF High-Altitude Partial Pressure Protective Assembly," NASA TM-72864, 1979.

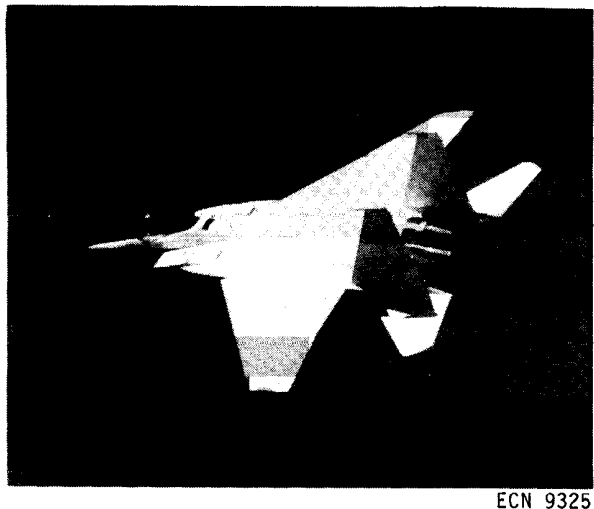


Fig. 1 F-15 airplane in flight.

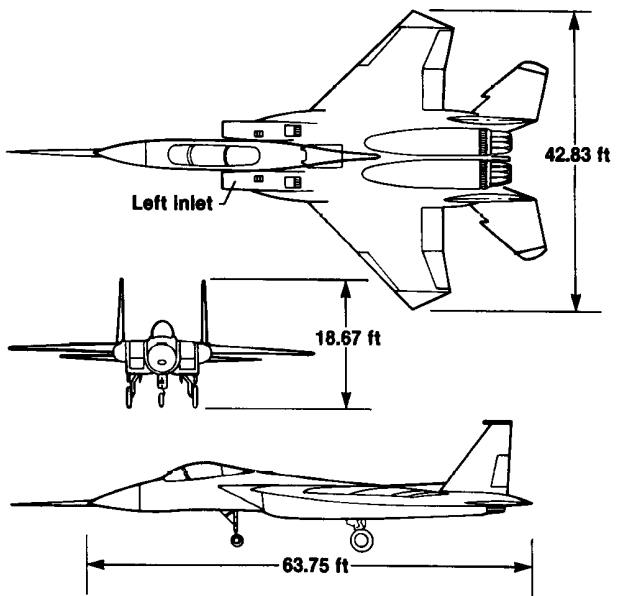


Fig. 2 Three-view of test airplane.

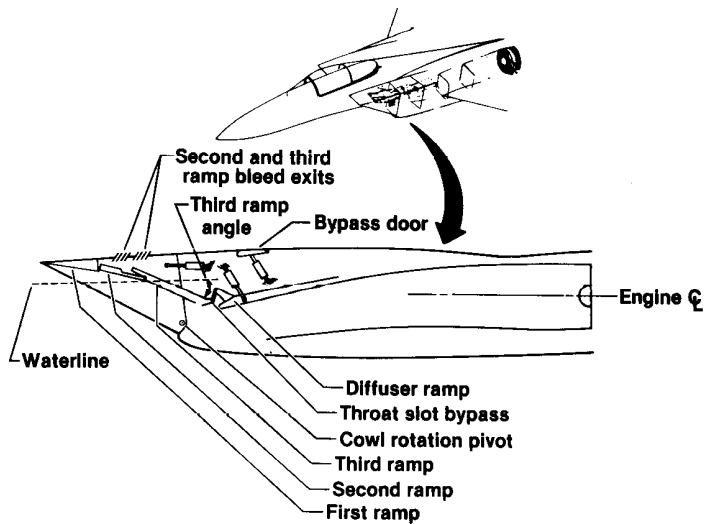


Fig. 3 F-15 inlet.

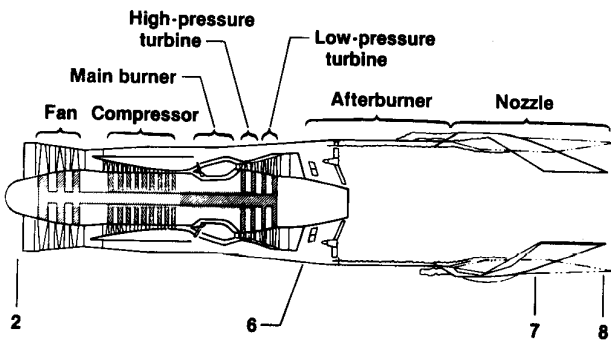


Fig. 4 F100 engine and stations.

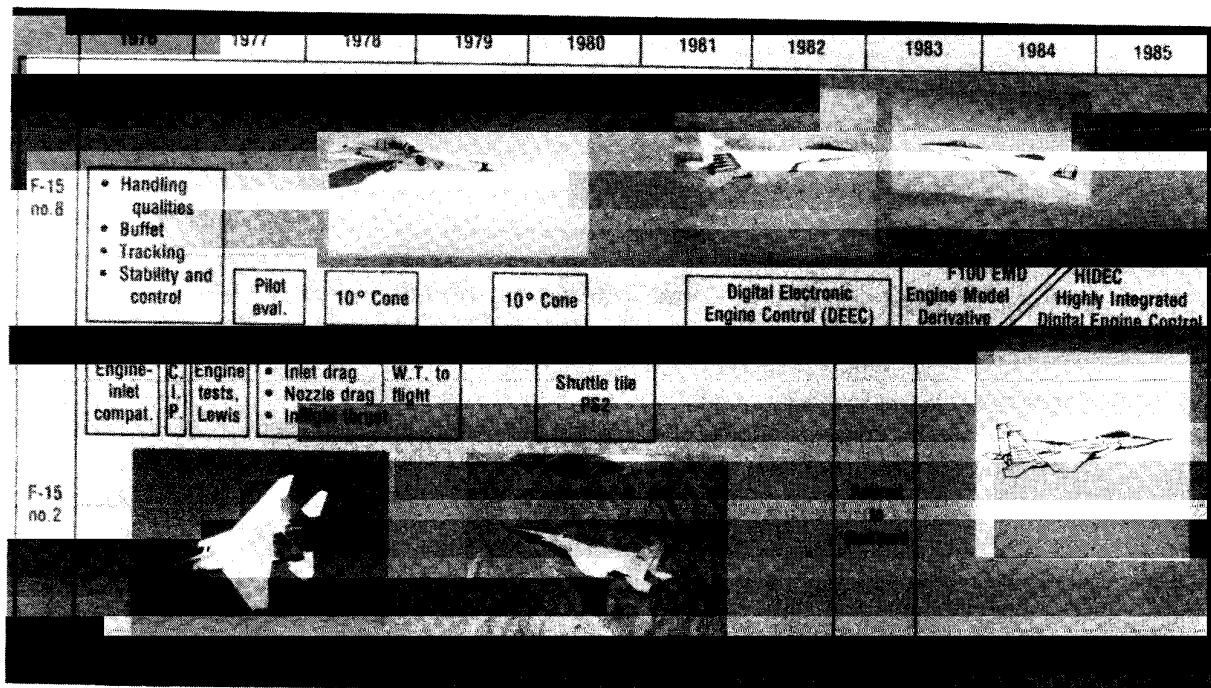
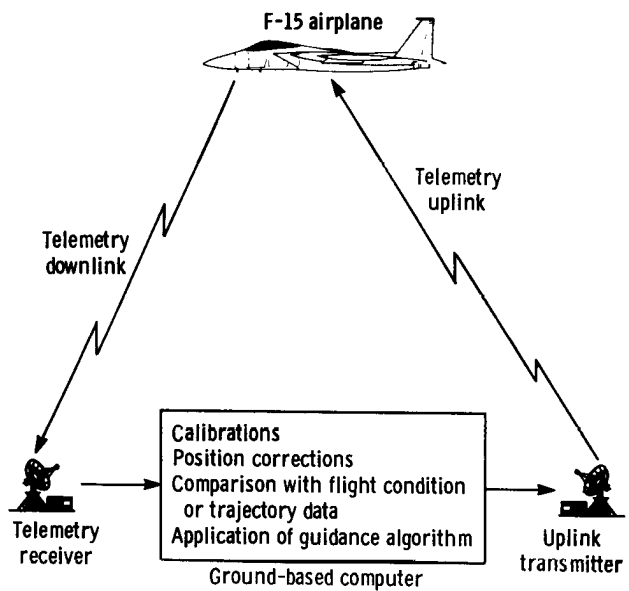
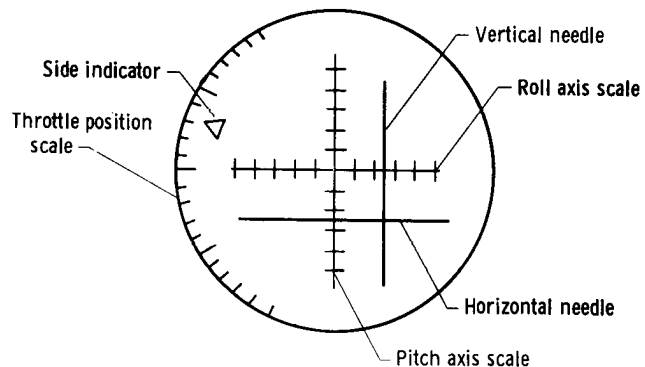


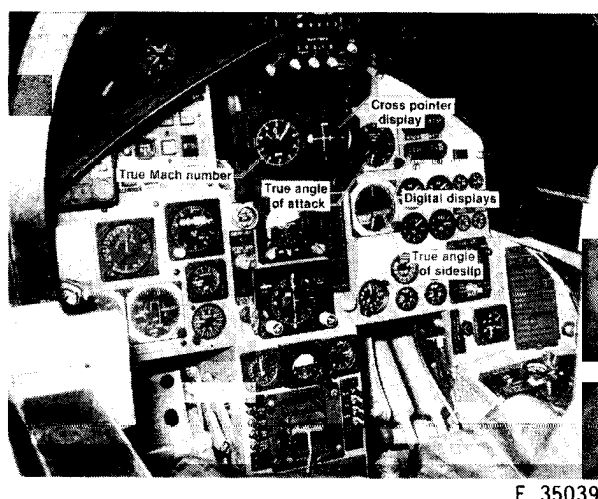
Fig. 5 Summary of major F-15 flight research projects.



(a) Schematic view of flight test trajectory guidance system.

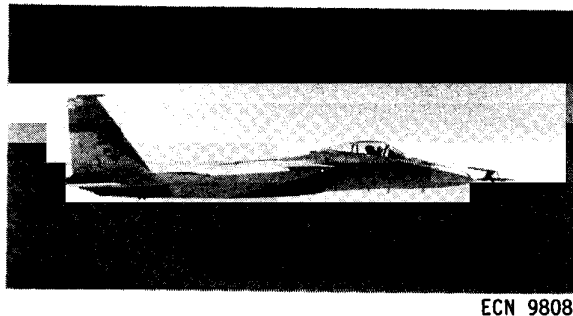


(b) Generic pilot display device.

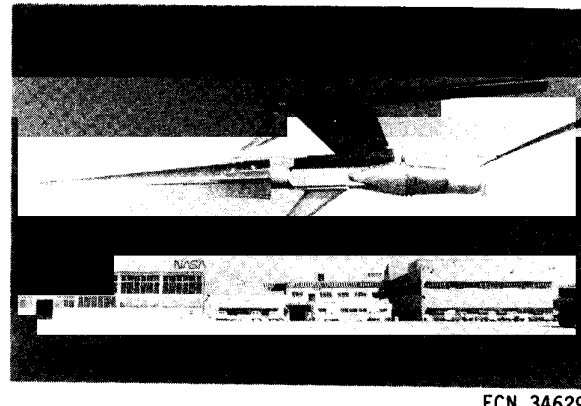


(c) F-15 cockpit showing cockpit uplink displays.

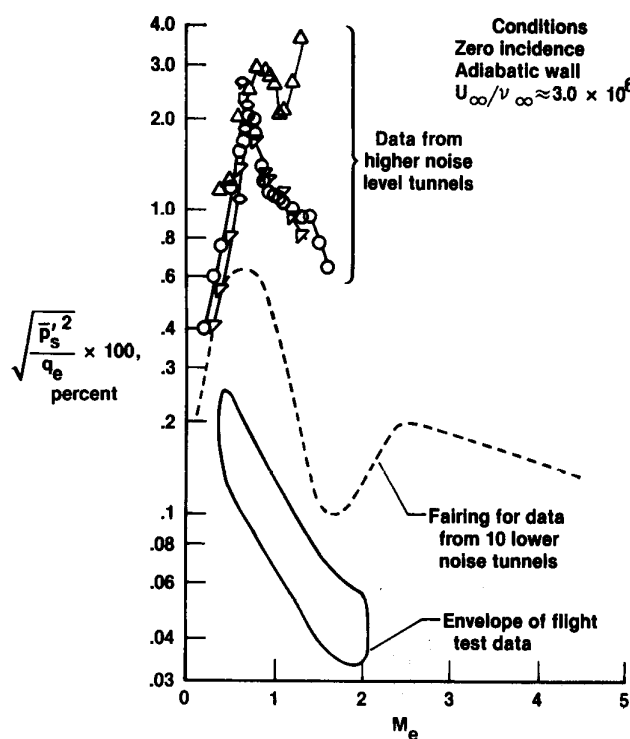
Fig. 6 Flight test trajectory guidance system used in F-15 airplane.



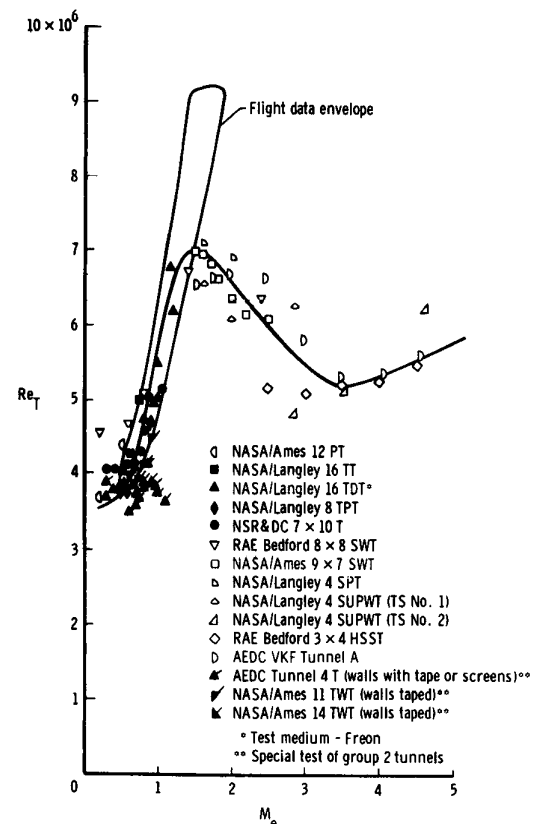
(a) F-15 airplane with 10-deg cone installed.



(b) Closeup of 10-deg cone.

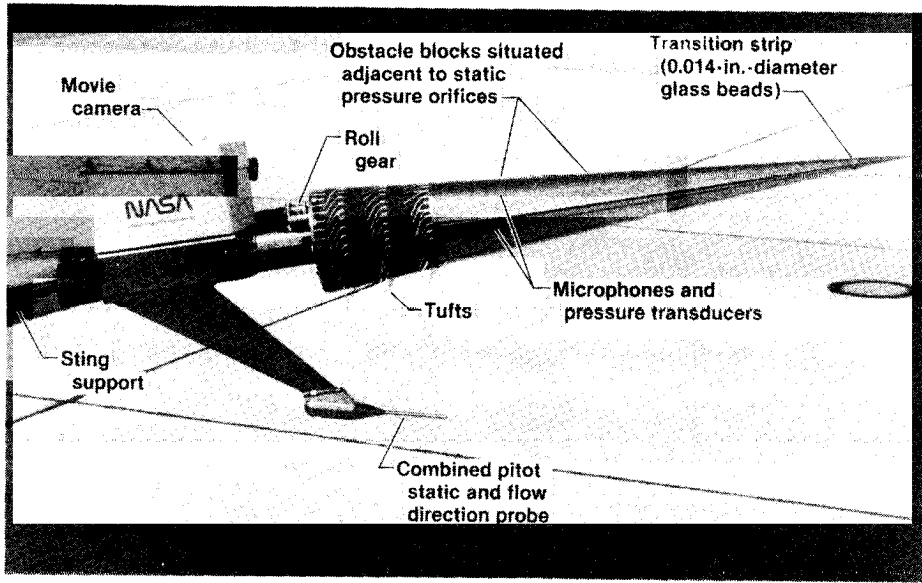


(c) Comparison of disturbance levels measured in wind tunnels with those measured in flight.



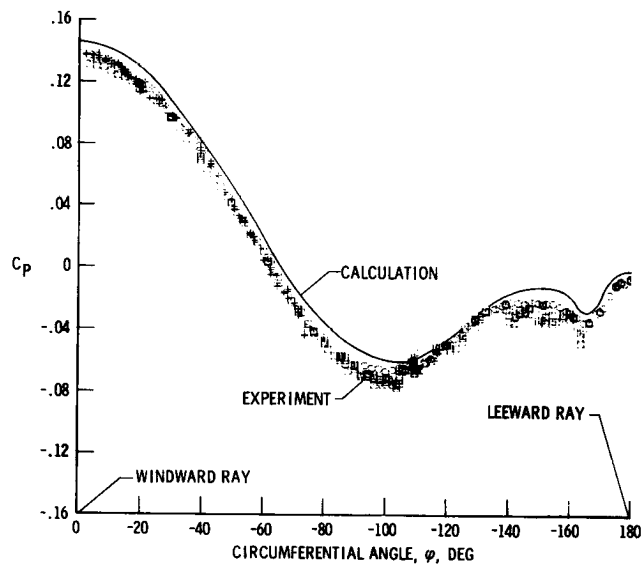
(d) Comparison of transition Reynolds number with Mach number for flight and lower noise wind tunnels, $Re = 3.0 \times 10^6/\text{ft}$ (from Ref. 18).

Fig. 7 Summary of results from 10-deg transition cone experiment.

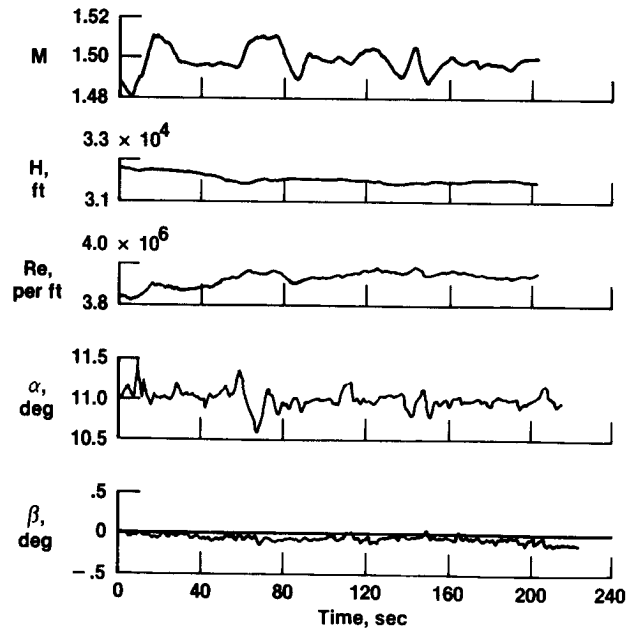


E 37308

(a) 10-deg cone at 11-deg incidence.

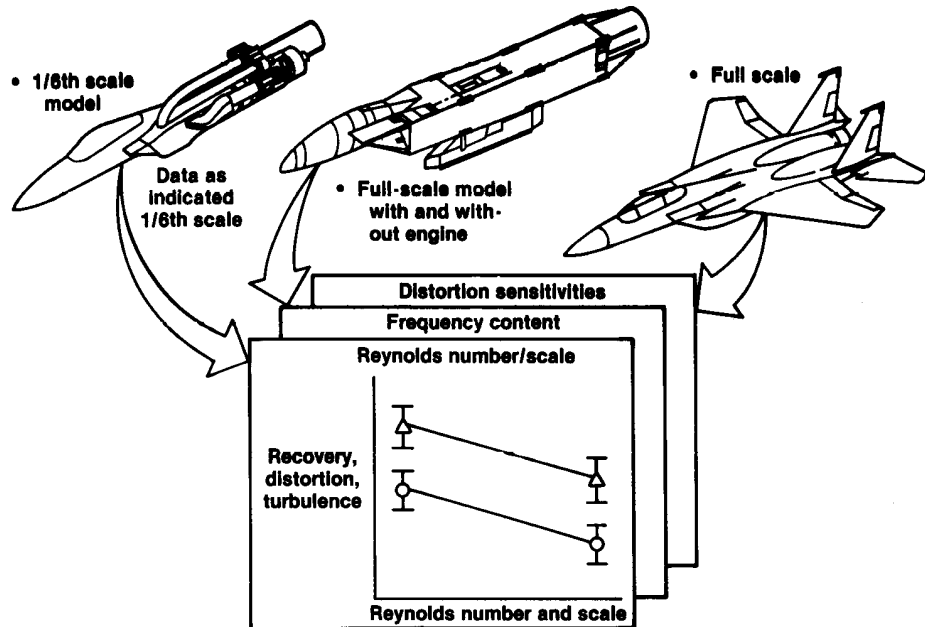


(b) Flight results, $Re = 4.0 \times 10^6/\text{ft}$.

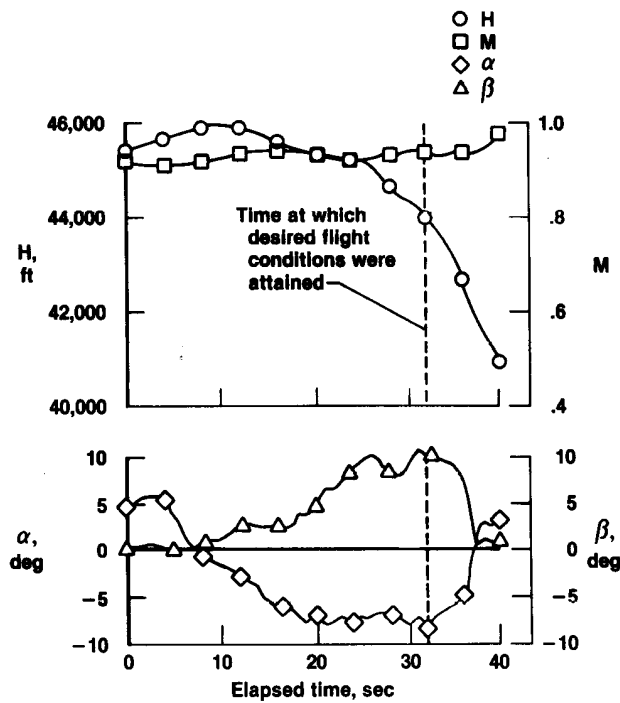


(c) Time history of typical F-15 cone experiment maneuver.

Fig. 8 10-deg cone separation experiment.

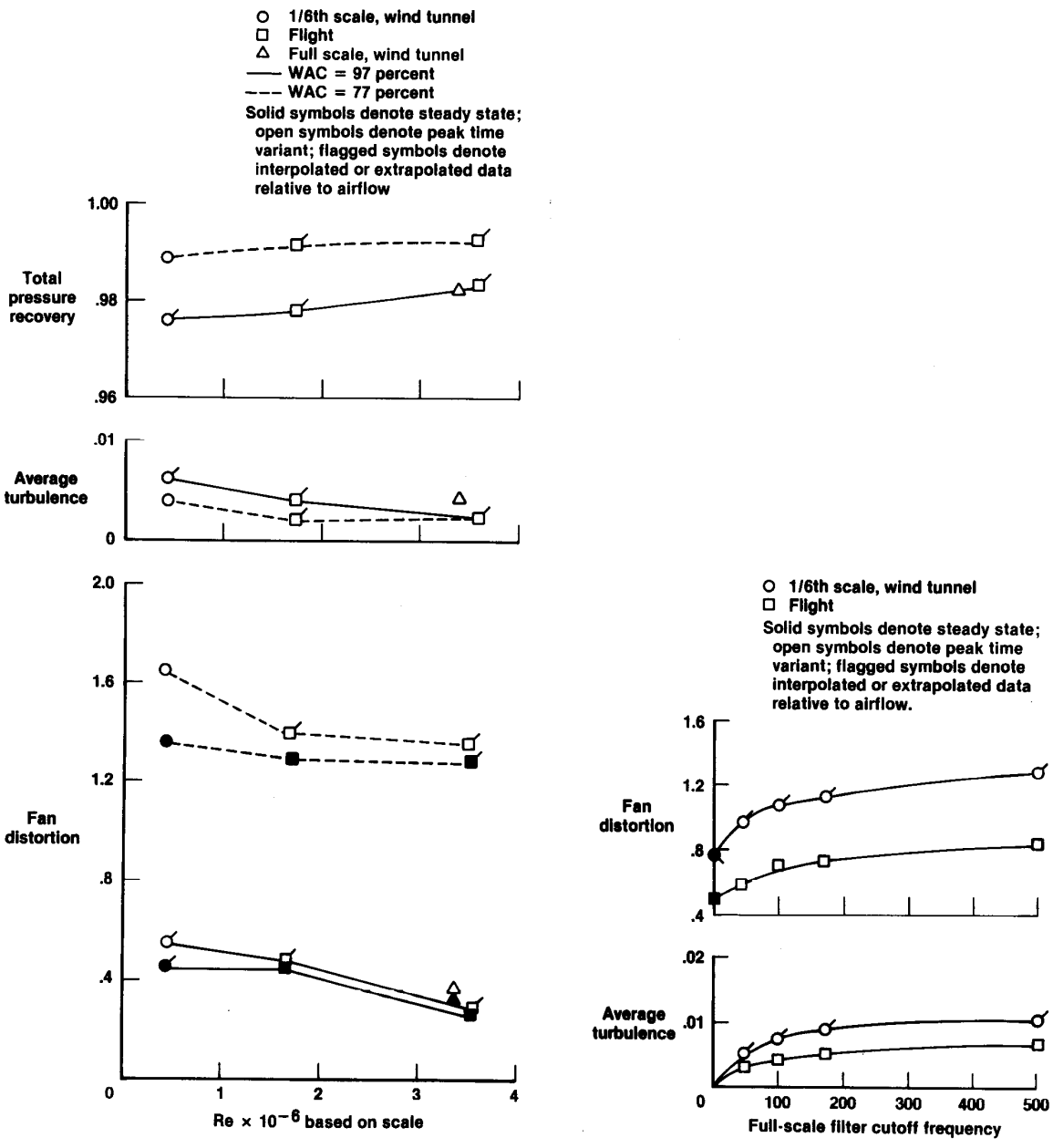


(a) One-sixth scale wind tunnel, full-scale wind tunnel, and flight data sources.



(b) Extreme flight test maneuver.

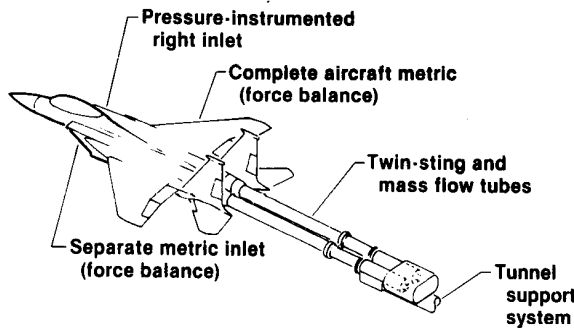
Fig. 9 Engine-inlet compatibility research project.



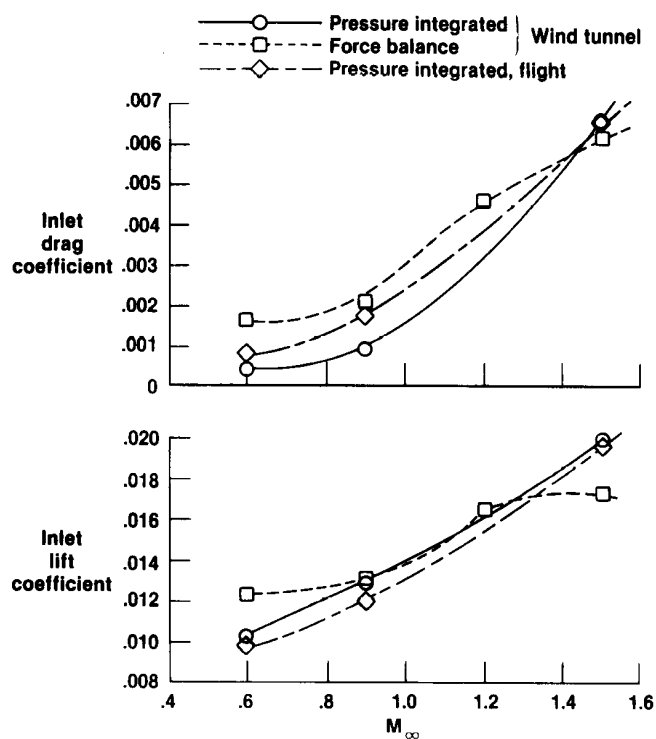
(c) Effect of Reynolds number and scale on total pressure recovery, turbulence, and fan distortion, $M = 0.6$, $\alpha = 4$ deg, and $\beta = 0$ deg.

(d) Effect of filter cutoff on fan distortion and turbulence, $M = 1.8$, $\alpha = -2$ deg, $\beta = 0$ deg, and WAC = 80.7 percent.

Fig. 9 Concluded.

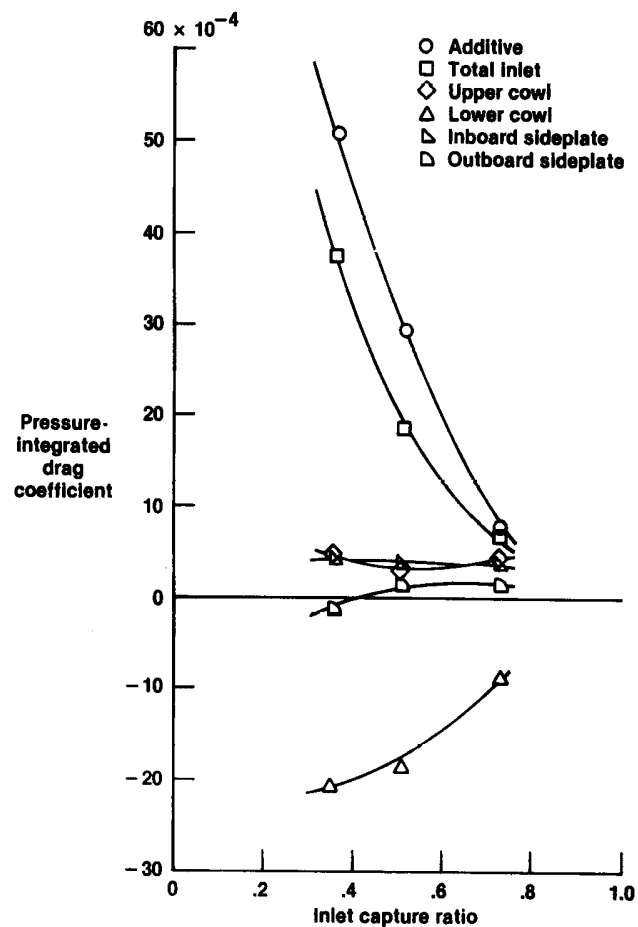


(a) Inlet model twin force balance sting system.



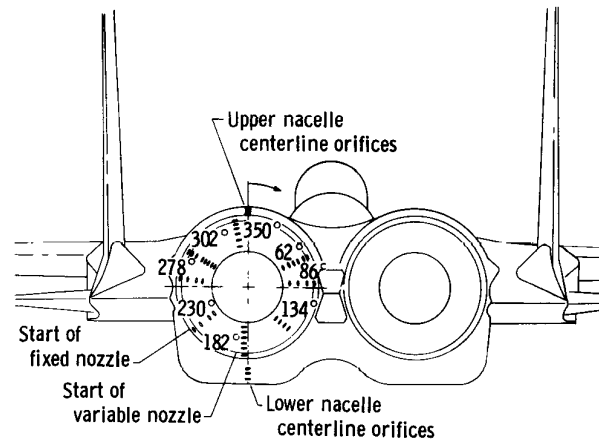
(b) Variation of inlet lift and drag with Mach number,
 $\alpha = 5$ deg.

Fig. 10 Inlet-airframe integration research project.

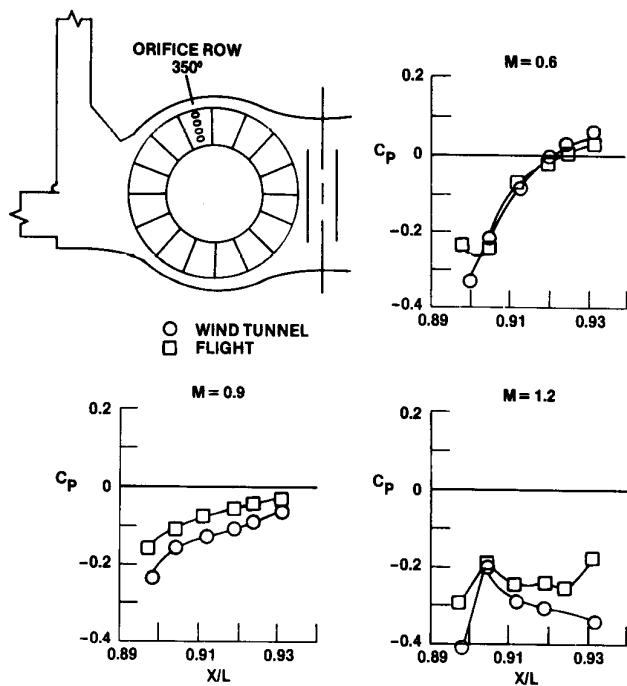


(c) Typical pressure integrated inlet drag components from F-15 flight data.

Fig. 10 Concluded.

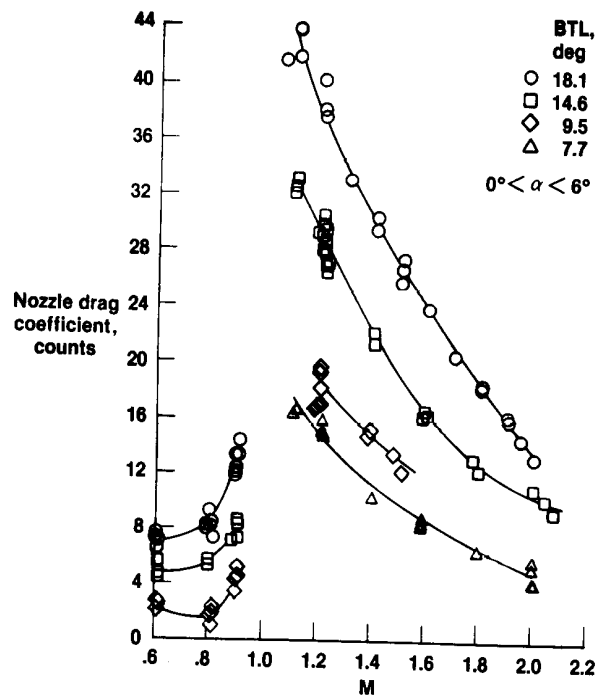


(a) Afterbody surface pressure instrumentation.

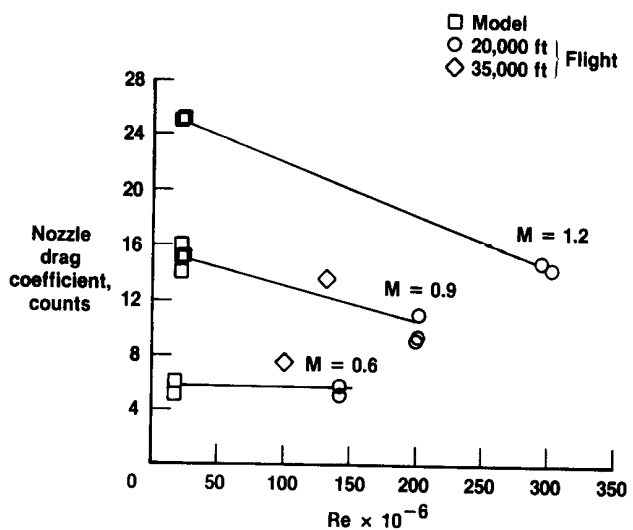


(b) Nozzle surface pressure coefficient.

Fig. 11 Nozzle and aft engine integration research project.

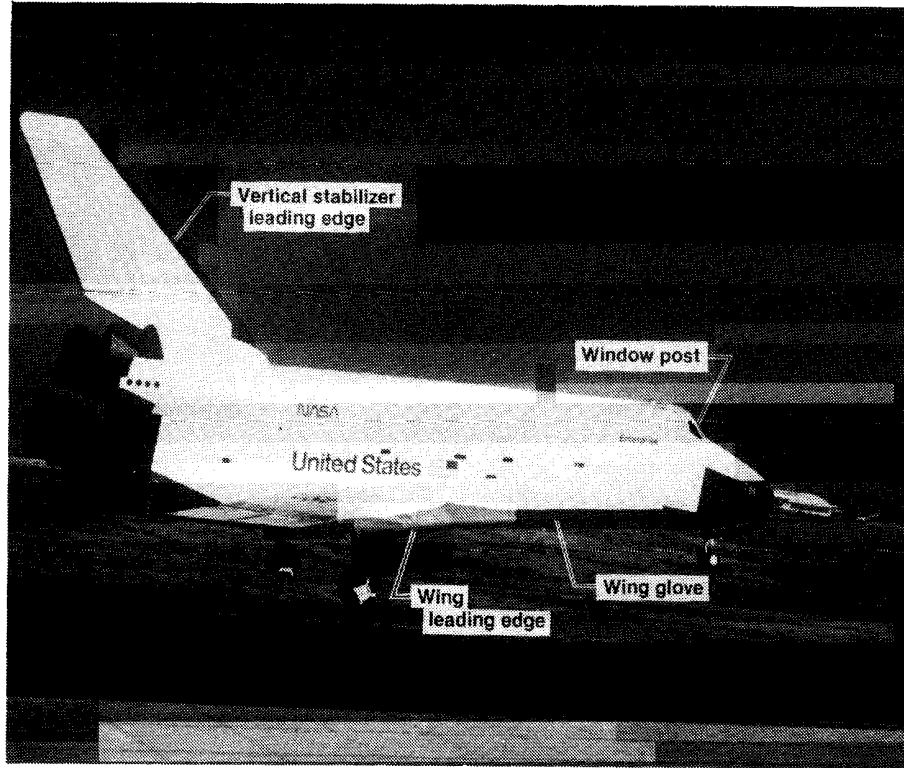


(c) Flight nozzle drag as a function of Mach number.



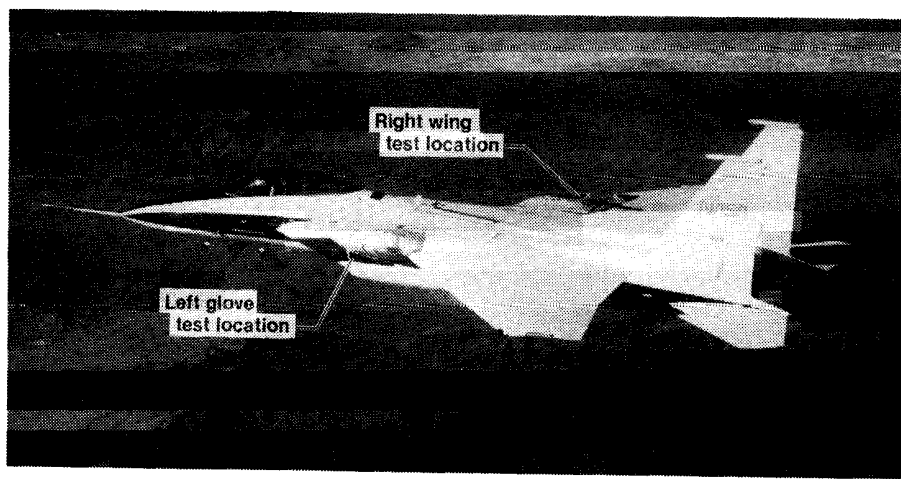
(d) Nozzle drag as a function of Reynolds number.

Fig. 11 Concluded.



ECN 9082

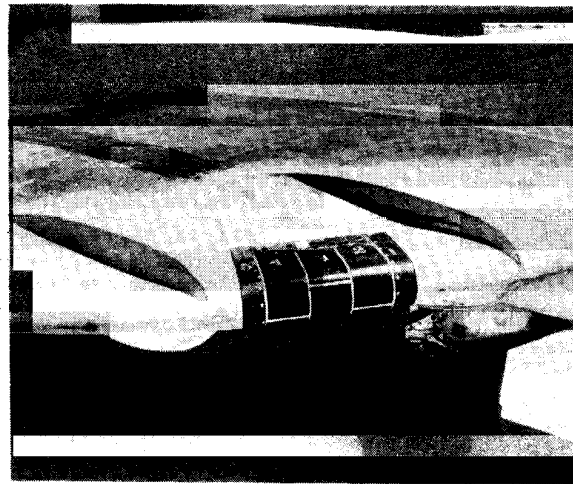
(a) Shuttle thermal protection system areas tested.



E 36697

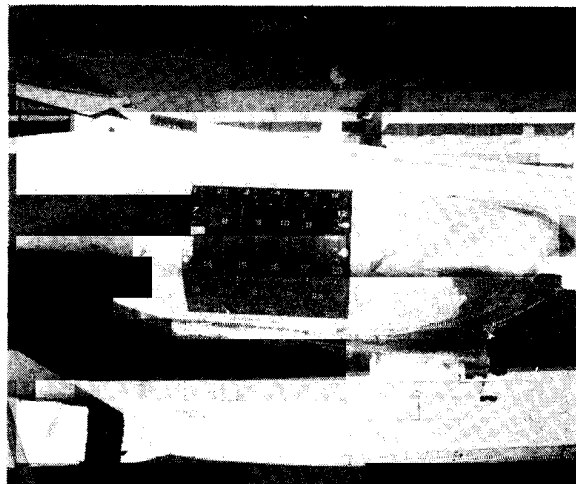
(b) Airplane with test articles mounted in right wing and left glove locations.

Fig. 12 Space shuttle thermal protection system evaluation on F-15A-2 airplane.



ECN 13387

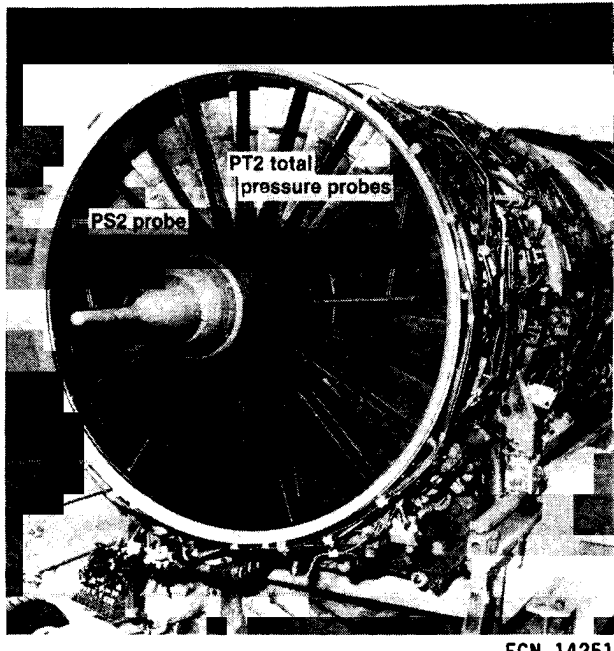
(c) Shuttle vertical stabilizer leading edge
test article mounted on F-15A-2 right wing.



ECN 13386

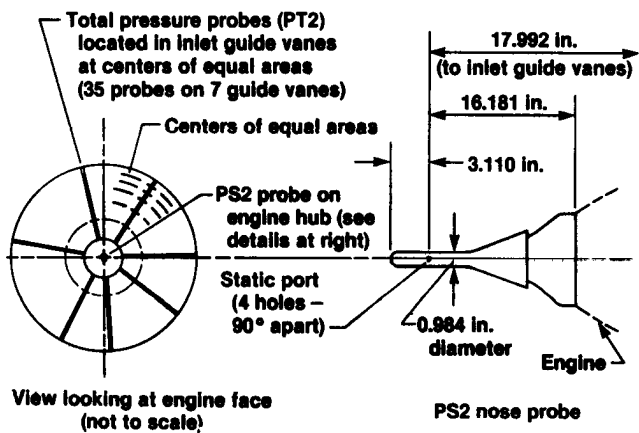
(d) Shuttle wing glove test article mounted on
F-15A-2 left wing glove (side view).

Fig. 12 Concluded.

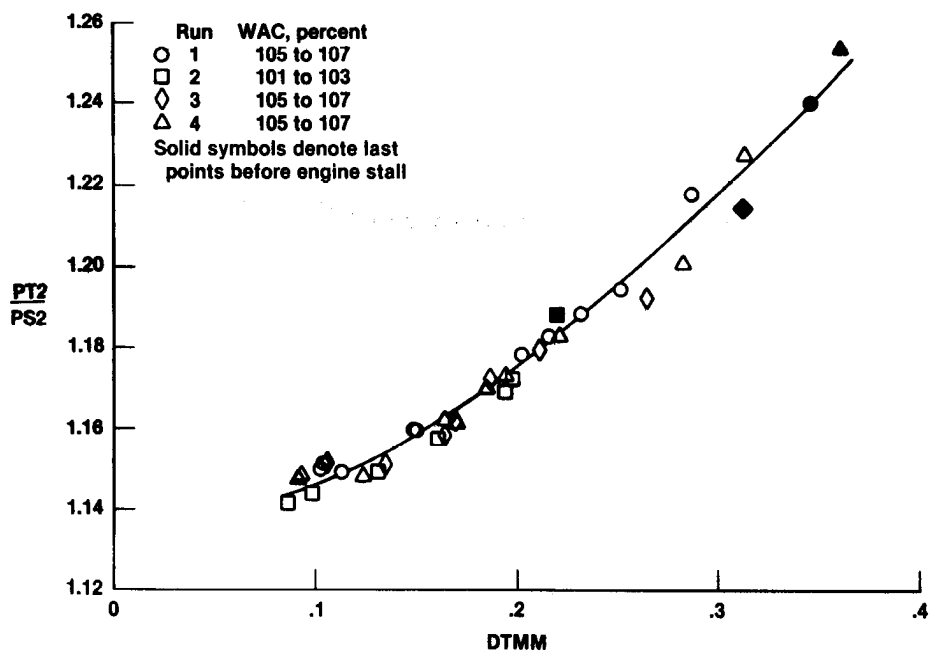


ECN 14251

(a) Engine-inlet static pressure (PS2) and fan inlet total pressure (PT2) probes at engine face.

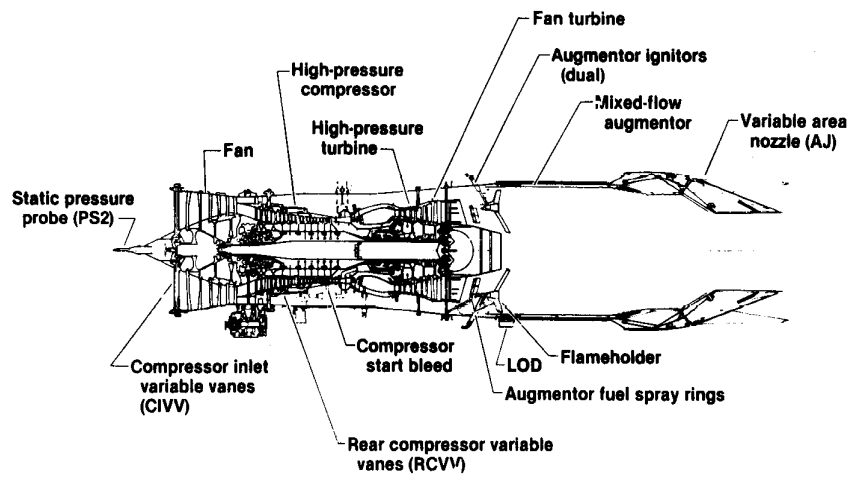


(b) Engine-inlet pressure instrumentation.

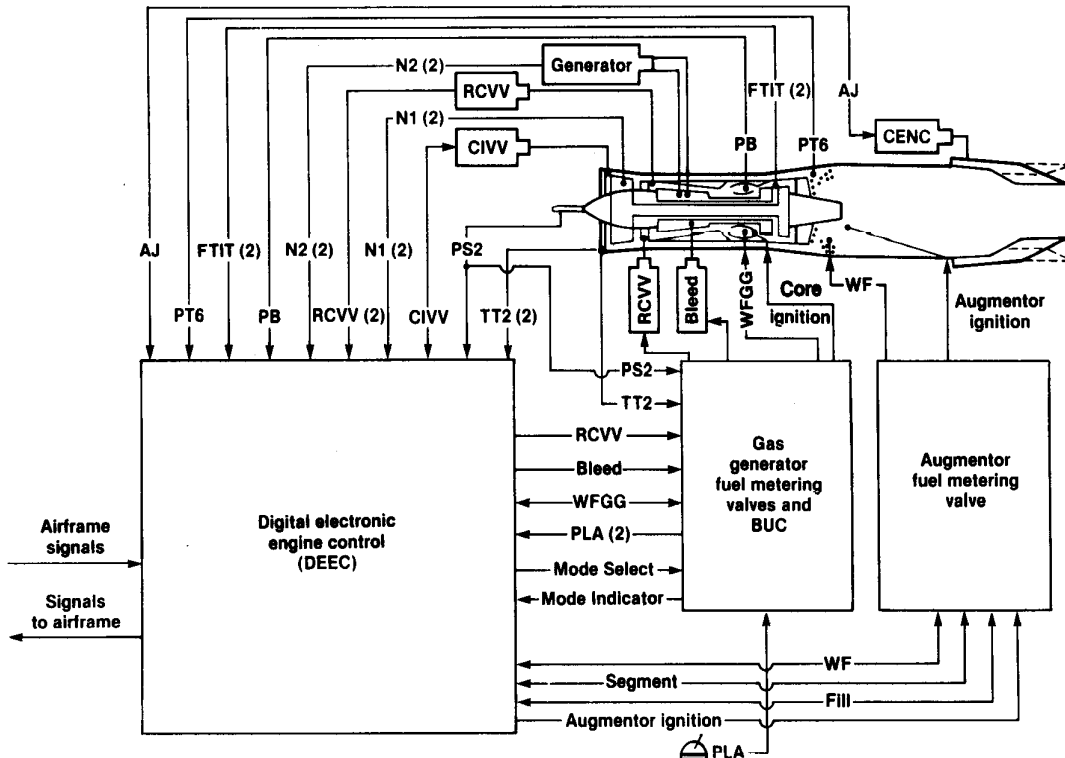


(c) Maximum-minimum total pressure distortion factor.

Fig. 13 Engine-inlet static pressure experiment.

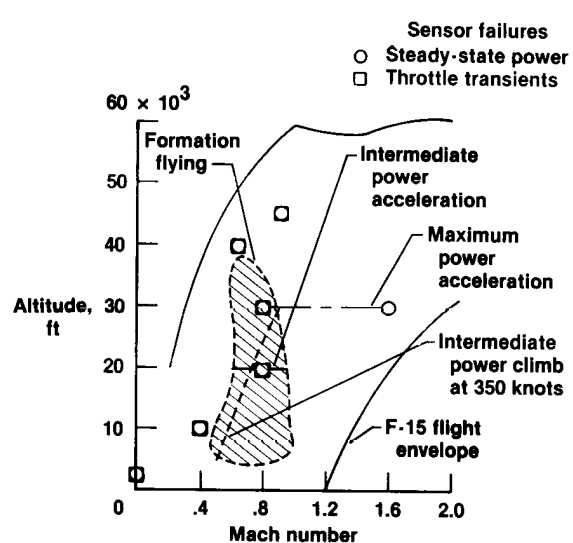
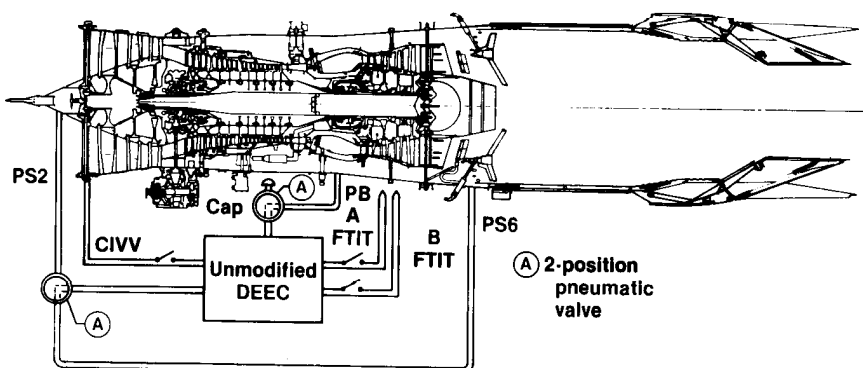
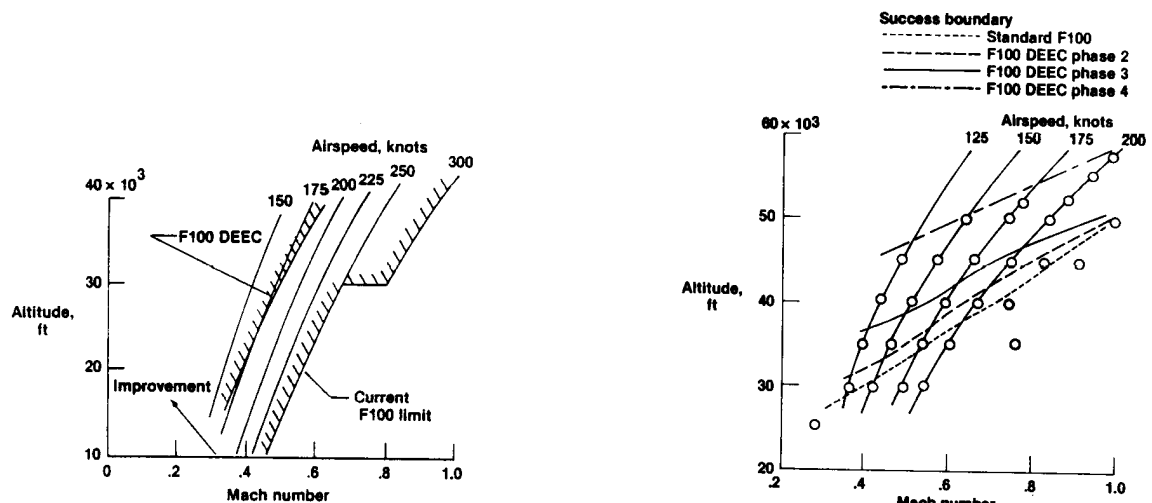


(a) Section view of F100 engine used in flight evaluation.



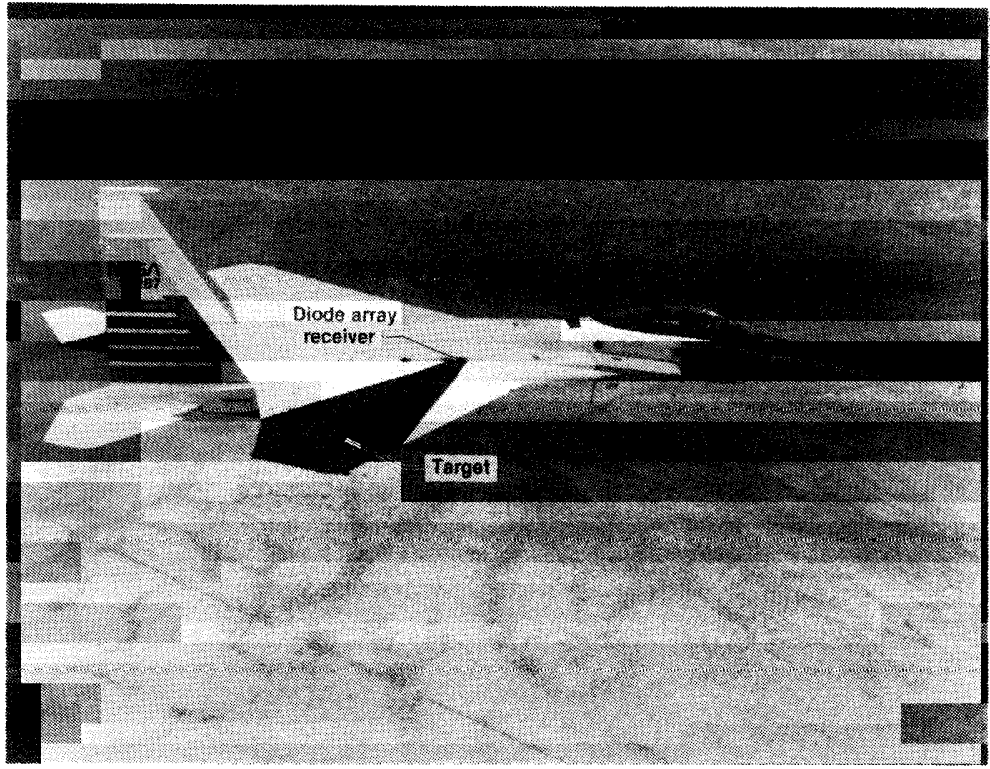
(b) DEEC system diagram.

Fig. 14 DEEC research project.



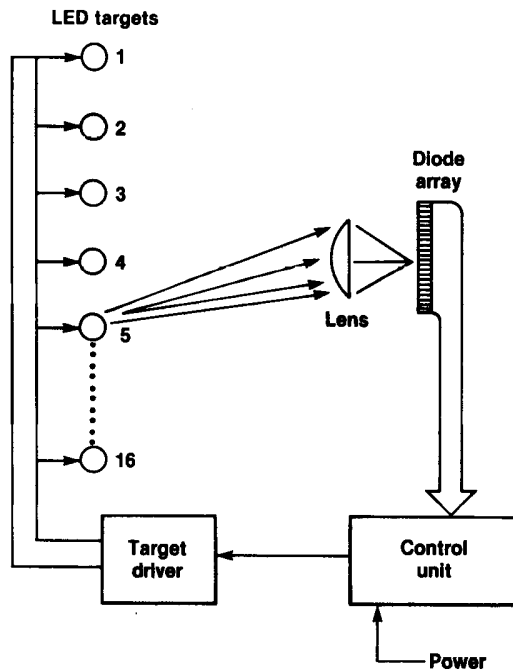
(f) Fault detection and accommodation test points.

Fig. 14 Concluded.



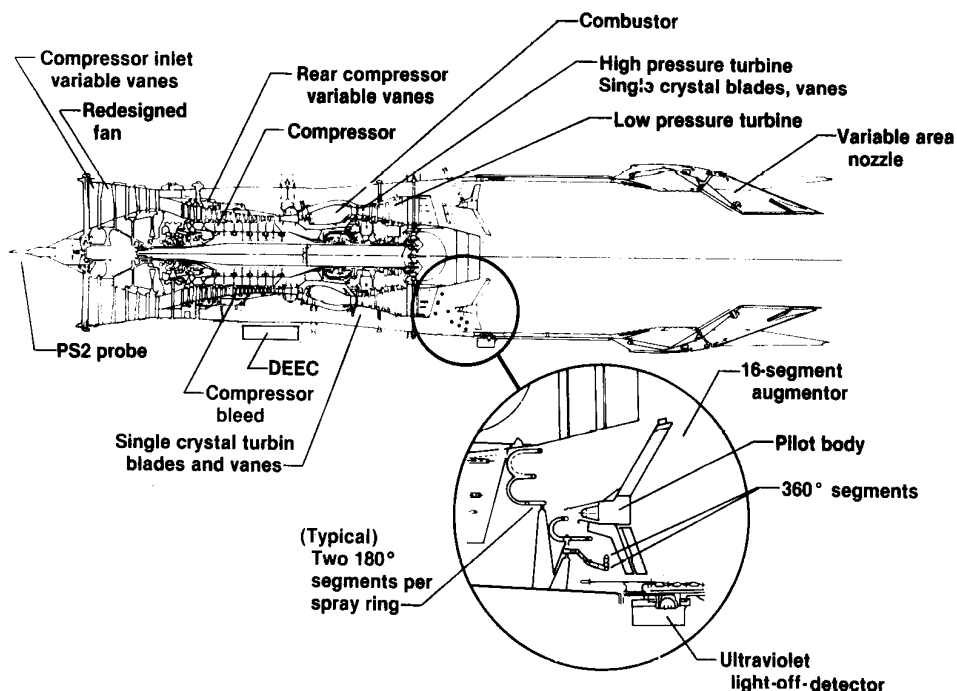
ECN 18894

(a) F-15A-8 airplane with deflection measuring system installed on right wing.

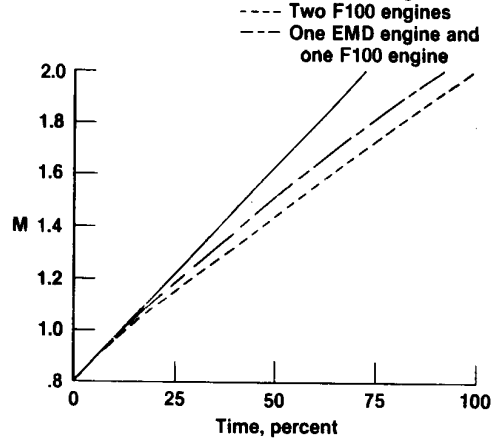


(b) Deflection measuring system schematic.

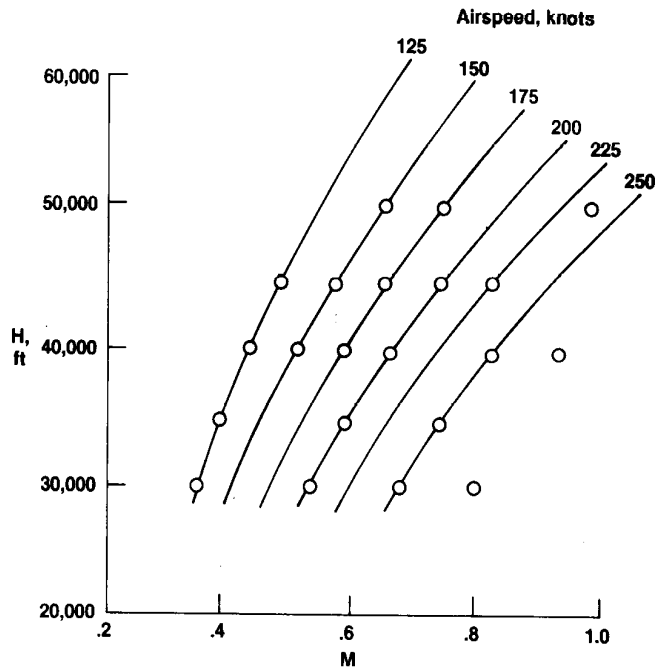
Fig. 15 Deflection measuring system evaluation.



(a) Section view of engine showing advanced features.

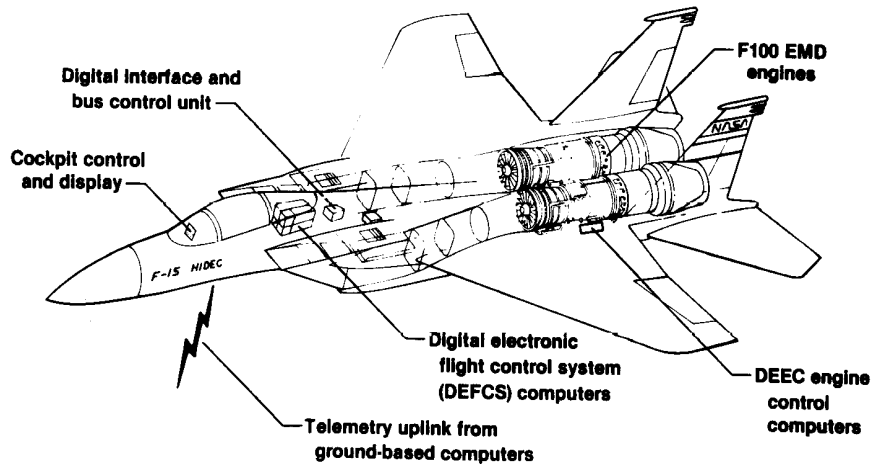


(b) Comparison of 40,000-ft level accelerations at maximum power and standard day conditions.

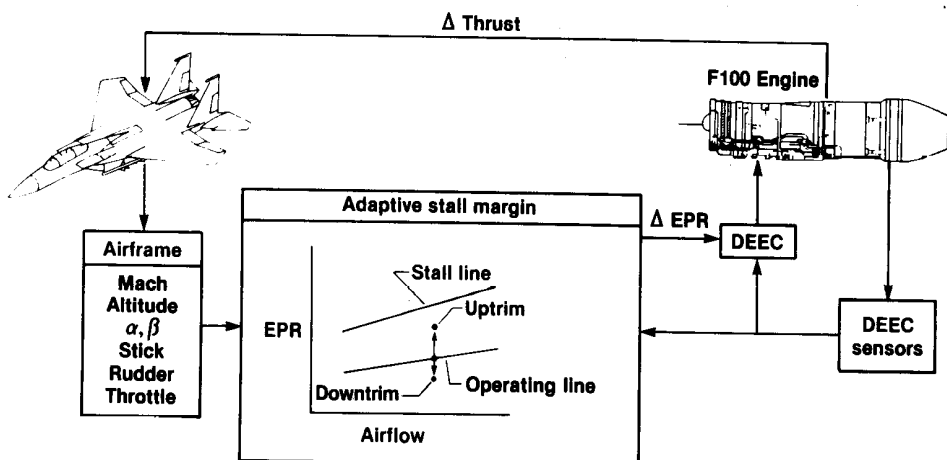


(c) Successful idle-to-maximum power throttle transients.

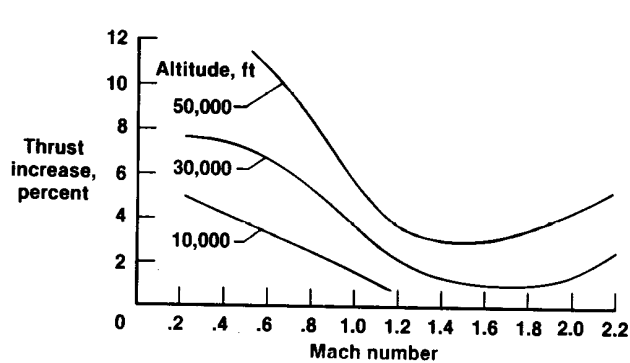
Fig. 16 F100 EMD evaluation.



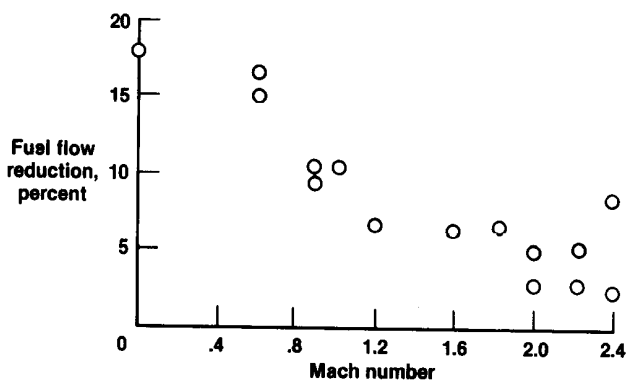
(a) Features of F-15 HIDECE research airplane.



(b) ADECS.



(c) Predicted thrust increase for ADECS mode at maximum power.



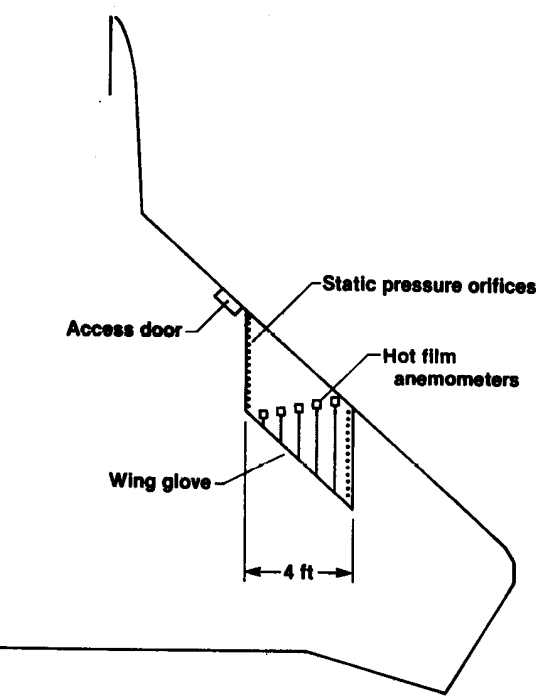
(d) Predicted reduction in fuel flow with engine pressure ratio uptrim to obtain nonuptrimmed maximum thrust.

Fig. 17 HIDECE project.



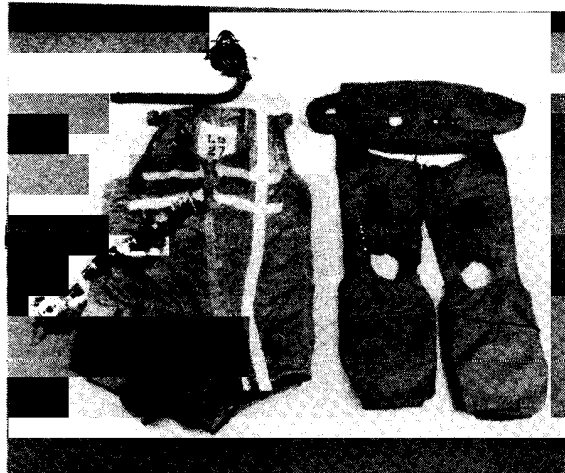
ECN 33330-005

(a) Supersonic laminar flow glove.



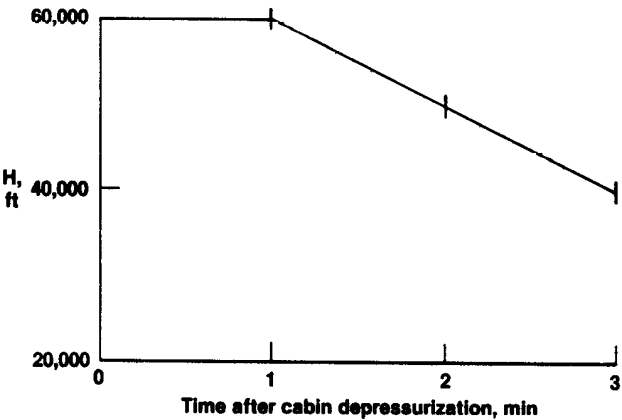
(b) Wing glove showing instrumentation.

Fig. 18 Supersonic laminar flow experiment.



ECN 9181

(a) Pressure jerkin and dual-bladder anti-gravity suit trousers.



(b) Pressure jerkin altitude envelope.

Fig. 19 Royal Air Force high-altitude partial pressure protective assembly.

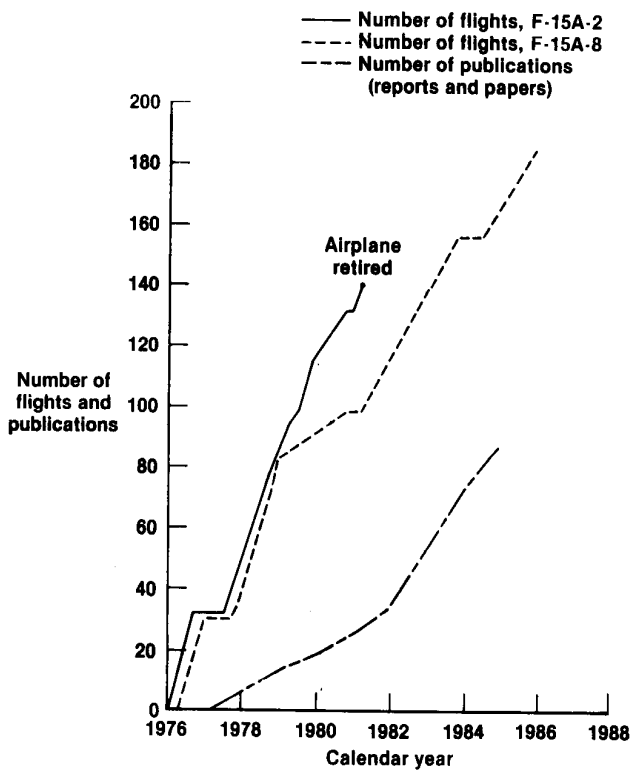


Fig. 20 F-15 research program flight and publication rates.

*For sale by the National Technical Information Service, Springfield, Virginia 22161.